Characterization and Stabilization of a High Power Fiber Amplifier Laser

Von der Fakultät für Mathematik und Physik
der Gottfried Wilhelm Leibniz Universität Hannover

genehmigte Dissertation

zur Erlangung des Grades
Doktor der Naturwissenschaften
Dr. rer. nat.

Dipl.-Phys. Patrick Oppermann

2017

Abstract

High power lasers are required for interferometric experiments, such as the search of gravitational waves. Besides the high power, excellent beam parameters are essential.

The experiments at the AEI 10 m prototype require up to 8 W of stabilized laser power. Therefore, the design and installation of the 35 W Enhanced LIGO (eLIGO) amplifier, the photonic crystal fiber, the mode cleaner and the power stabilization is described. For power stabilization the aLIGO photo diode array was installed and the stabilization to a relative power noise of $2 \times 10^{-9} / \sqrt{\text{Hz}}$ was demonstrated.

High power, low noise, fundamental spatial mode, single-frequency lasers are required for gravitational wave detectors. Solid state amplifiers have been used for this purposes for decades. A possible laser amplifier for aLIGO, amplifying up to 70 W, was analyzed and installed in the aLIGO reference system.

For future interferometric gravitational wave detectors, lasers with an output power of up to 500 W are required. Fiber amplification appears to be a promising candidate. Besides total optical power, also the power noise, frequency noise, beam pointing fluctuations, and spatial beam parameters have to meet strict requirements. In collaboration with the Laser Zentrum Hannover, a two stage fiber amplifier was developed. The resulting output power is comparable to the high power oscillator and delivers up to 180 W. The technical feasibility of a long term stable single frequency amplifier without photo-darkening or stimulated Brillouin scattering was shown. The system has a similar performance in frequency noise and spatial beam parameters as the aLIGO free running laser. The power noise and beam pointing fluctuation are better than with the aLIGO laser.

Key words: <Fiber Amplifier, single-frequency lasers, Advanced LIGO photo diode array>

Zusammenfassung

Für laserinterferometrische Experimente wie zum Beispiel die Suche nach Gravitationswellen werden Hochleistungslaser benötigt. Neben hoher Leistung sind exzellente Stahlparameter essenziell.

Die Experimente am AEI 10 m Prototyp benötigen bis zu 8 W stabilisierten Laserlichts. Dafür wird der Aufbau und die Installation des 35 W Enhanced LIGO (eLIGO) Verstärkers, der Photonischen Kristallfaser, des optischen Resonators zum unterdrücken der Lasermoden und der Leistungsstabilisierung beschrieben. Zur Leistungsstabilisierung wurde das Advanced LIGO (aLIGO) Photodioden-Array installiert und die Stabilisierung auf ein relatives Leistungsrauschen von $2 \times 10^{-9} / \sqrt{\text{Hz}}$ demonstriert.

In Gravitationswellendetektoren werden ebensolche Hochleistungslaser verwendet. Diese müssen rauscharm, schmalbandig und in der transversalen Grundmode sein. Für diese Zwecke werden seit Jahrzehnten Festkörperverstärker verwendet. Ein möglicher Laserverstärker für aLIGO, der bis zu einer Ausgangsleistung von 70 W verstärkt, ist im aLIGO Referenz System installiert und analysiert worden.

Für zukünftige interferometrische Gravitationswellendetektoren werden Laser mit einer Ausgangsleistung von bis zu 500 W benötigt. Faserverstärkung erscheint als ein vielversprechender Kandidat. Neben der gesamten optischen Leistung müssen auch das Leistungsrauschen, das Frequenzrauschen, die Strahllagefluktuationen und die Strahlparameter strengen Anforderungen genügen. In Zusammenarbeit mit dem Laser Zentrum Hannover wurde ein zweistufiger Faserverstärker entwickelt. Die resultierende Ausgangsleistung ist vergleichbar mit dem aLIGO Hochleistungsoszillator und liefert bis zu 180 W. Die technische Realisierbarkeit eines langzeitstabilen schmalbandiger Laserverstärkers ohne Materialalterung oder stimulierte Brillouin Streuung wurde gezeigt. Das System hat eine ähnliche Leistung im Frequenzrauschen und den räumlichen Strahlparametern wie der unstabilisierte aLIGO-Laser. Das Leistungsrauschen und die Strahllagefluktuation sind hingegen deutlich besser als beim aLIGO-Laser.

Table of contents

List of figures

Chapter 1

Introduction

The detection of gravitational waves in September 2015 started the era of gravitational wave astronomy [1]. The hunt for gravitational waves was successful after all, due to decades of innovations and developments of the interferometric detectors. A major key in making the detectors stable enough for the detection of gravitational waves, was the development of their laser light sources and their stabilization concepts. This was crucial, since gravitational wave detectors set most stringent requirements for laser output power, power and frequency stability, as well as the spatial beam profile.

The aLIGO detectors use a laser system consisting of a 2 W 1064 nm NPRO (Non-Planar-Ring Oscillators), which is amplified in two stages. The first stage is provided by a solid state crystal amplifier delivering 35 W output power. It is seeded with the NPRO to maintain the good noise performance. In a second stage the light is coupled into an injection locked high-power ring oscillator with four diode pumped Nd:YAG crystals. In this way 180 W of output power are generated. The laser beam is then stabilized with passive and active stabilization techniques to meet the stability requirements at the input of the detectors.

Future Gravitational wave detectors, like the Einstein Telescope, will need an optical power of around 500 W [36]. The current amplification concepts can not be scaled up to higher output power, due to technical problems. Therefore new laser amplification concepts have to be investigated.

The thesis will start with an overview of the aLIGO laser and its initial stabilization concepts, in the second chapter. Chapter three will discuss, an improved version of the stabilization concept, which was integrated into the AEI 10 m Prototype Interferometer [13]. The fourth chapter will discuss the limitations of common solid state amplifiers and

show a state of the art 70 W amplifier. The last chapter is focusing on a completely new approach for the generation of high output powers, an all fiber based amplifier concept developed in close cooperation with the LZH.

Chapter 2

Stabilized Lasers for current and future Gravitational Wave Detectors

Gravitational wave detection is one of the most demanding measurements, requiring high laser power, in combination with excellent power and frequency stability as well as excellent spatial beam profile. The current generation of gravitational wave detectors is using between 35 W at the GEO600 [2] detector up to 200 W of laser output power at the Advanced LIGO detectors (aLIGO) [21, 12]. The Einstein Telescope is one of the planed detectors for the third generation. The interferometric readout is split into high and low frequency interferometers, called ET-LF and ET-HF. The high frequency interferometers will be using light of 1064 nm wavelength, as in all current detectors. The output power of the laser will be raised up to 500 W.
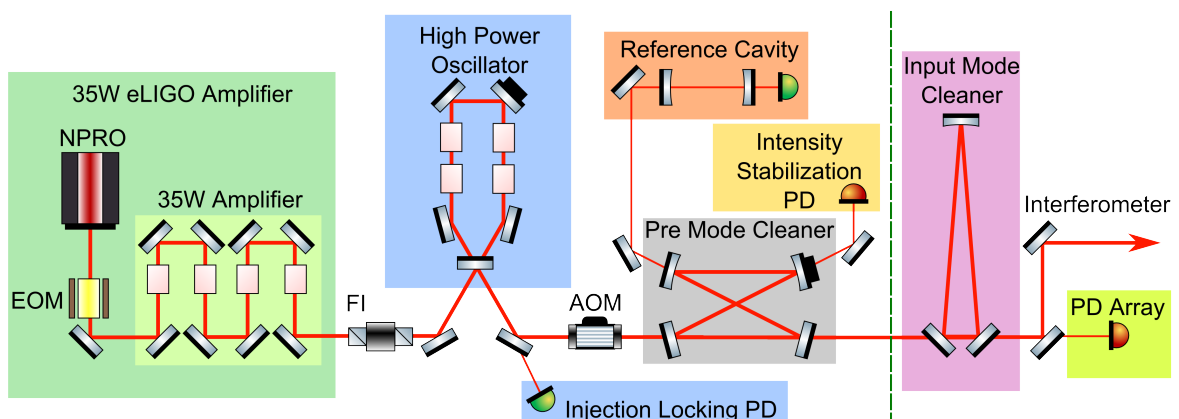
Fig. 2.1 Setup of the aLIGO pre stabilized laser system.

2.1   Advanced LIGO

In autumn 2015 the major upgrade of the LIGO detectors was completed [38] and the first science run was started. The upgrade included new mirrors and seismic isolation [14], signal recycling and an upgrade of the laser system. An High Power Oscillator (HPO) was installed. It is seeded with the Enhanced LIGO [10] 35 W laser amplifier and provides 200 W output power [19]. During the first science runs the sensitivity will be gradually increased, mainly by raising the input power to the interferometer. In the last step a squeezed light source will be installed, to reduce the shot noise [26]. The new lasers for aLIGO as well as the stabilization were developed in Hanover. Therefore several prototypes of the laser were developed in the LZH and the final System was setup at the AEI in Hanover. This Reference System consists of the 35 W eLIGO amplifier [10] and the 200 W high power oscillator [45]. A detailed description and the developed stabilization schemes will be explained in the following sections. A picture of the entire table layout is shown in Figure 2.1. The system consists of the 35 W eLIGO amplifiers , which provides actuators for power and frequency modulation. It is followed by the HPO, which can produce up to 200 W. A Faraday Isolator between eLIGO laser and HPO is used to avoid back reflections from the HPO. This power can be adjusted again with the high power AOM. The beam is then filtered by the a bow tie Pre Mode Cleaner (PMC) with two stabilization outputs at the curved mirrors. The power is stabilized with the ISS-PD. The frequency of the laser is stabilized to the reference cavity. This is followed by the input mode cleaner (IMC), behind which is the PD array.

2.1.1   35 W eLIGO Amplifier

The 35 W eLIGO laser consists of a NPRO seed laser and a four stage solid state amplifier. The whole amplifier unit was already used in Enhanced LIGO [10]. The NRPO has an output power of 2 W at a wavelength of 1064 nm [11], [17]. The active laser material is neodymium doped yttrium aluminum garnet, which is pumped by laser diodes at a wavelength of 808 nm. The frequency and power noise of the NPRO is very low and thus the optimum start to build a high power laser with very good noise characteristics. This light is amplified to 35 W by a four-head Neodymium-doped yttrium orthovanadate amplifier. It is pumped via fiber with four pump diodes at a wavelength of 808 nm. A electro-optical modulator and a acousto-optic modulator are placed in between the NPRO and the amplifier.

The EOM serves two purposes. It is used to imprint a modulation on the laser light, which is later used for the stabilization of the High power oscillator and the mode filter. It is also used as phase modulator for the frequency stabilization feedback control loop of the laser light to the reference cavity.

The internal AOM can be used as actuator for power stabilization. This is done at GEO600 and the AEI 10 m prototype. For this, some laser power with a modulation frequency of 80 MHz is shifted into the first order of the AOM. For the aLIGO laser a second AOM is installed behind the HPO.

2.1.2 High Power Oscillator

Downstream of the 35 W Amplifier the light is coupled into the high power oscillator [45]. The HPO is a ring laser consisting of four diode-pumped Nd:YAG crystals. Each crystal is pumped by seven pump diodes. The individual crystals are pumped via fiber bundles. To transfer the good frequency stability of the eLIGO laser to the HPO, the length of the oscillator is matched to the incoming light. To created the error signal for the Pound-Drever Hall method [5], side bands are generated by the EOM of the eLIGO laser. The Signal is read by a photo diode in reflection of the HPO and the feedback is applied to a piezo driven mirror inside the oscillator. The output of the system it over 200 W of 1064 nm laser light in the fundamental mode maintaining the frequency noise of the NPRO. To reduce the thermal load at the Nd:YAG crystals it is necessary to cool the crystals directly by turbulent water flow.

2.1.3 Stabilization of the laser

Four parameters need to be stabilized, power noise, frequency noise, pointing and spatial beam profile [44],[32],[28]. The first part of the stabilization concept is a pre mode cleaner (PMC) which is a passive four mirror ring resonator in bow-tie configuration, with two planar and two curved mirrors. The geometry of the mode cleaner filters higher order modes and therefore mainly transmits the TEM00 mode [31]. The optical path length is 2 m. To provide a stable reference the mirrors are glued to an aluminum spacer. The length of the mode cleaner is stabilized with the Pound-Drever-Hall technique [5]. A piezo electric transducer (PZT) is glued between one of the curved mirrors and the spacer. The two plane mirrors serve as an input and output mirror. The finesse of the cavity is 130 with an FSR of 150 MHz. The higher order mode content of the transmitted beam is reduced

form 4 % to 0.5 %. The two transmitted beams through the curved mirrors are used for frequency and power stabilization.

As a reference for the frequency a ridged spacer cavity is used. It is made out of a quartz glass material, to provide thermal stability. To isolated it from the environment it is suspended in an ultra high vacuum tank. For vertical isolation coil springs are used and from there on wire slings are running around the cavity, providing horizontal isolation. To damp the resonant frequency eddy current damping is used. The laser frequency is stabilized to the length of this cavity. The feedback is applied to three different actuators. At high frequencies, the electro-optic modulator of the eLIGO 35 W amplifier is used to act onto the phase of the laser light. It is located between NPRO and 35 W amplifier. In the mid frequency range the refractive index of the the NPRO crystal is modulated by a piezo directly pushing onto the crystal. For low frequencies, the temperature of the NPRO crystal is adjusted. The offset of the piezo signal is offloaded to the temperature actuator and by that kept at its operating point.

The power stabilization consists of two sensors [37]. The first sensor is located on an the laser table, using one of the transmitted beams of the pre mode cleaner. It is sufficient for the initial stabilization of aLIGO. For the full sensitivity of aLIGO, a relative power noise of $2 \times 10^{-9}/\sqrt{\text{Hz}}$ has to be achieved. Therefore a second sensor, consisting of an array of eight photo diodes is needed (see 3.2.3). Four are used as in loop and four as out of loop detectors. At LIGO the PD-Array is set up and currently under commissioning [24]. The development was done in the AEI, and build at LIGO. The AEI 10 m Prototype requires the same power stability and therefore a PD-Array was transfered to Hanover. The stabilization scheme was adapted and improved to achieve the required sensitivity [15].

2.2   Third Generation - Einstein Telescope

For future interferometric gravitational wave detectors lasers with an output power of up to 500 W are required [36]. Instead of solid-state laser systems, fiber amplifier seem to be a promising candidate. In cooperation with the LZH a high power fiber amplifier was developed. To achieve an output power of 180 W, two fiber amplification stages are used. The seed laser for the first stage, the pre amplifier, is a 2 W NPRO. The light is amplified to 20 W by two fiber coupled pump diode, each with 25 W. The next stage, the main amplifier, is pumped by up to four diode. Each individual diode can deliver up to 100 W of output power with a wavelength of 976 nm.

For frequency stabilization the same scheme as in aLIGO is used. The power stabilization has four different actuators. Modulation of the NPRO pump current, an electro-optic amplitude modulator (EO-AM) in between the NPRO and the pre amplifier and two current shunts, one for each fiber amplifier stage.

Chapter 3

A stabilized Light source for the AEI 10 m Prototype

A 10 m prototype Michelson interferometer is currently being set up at the AEI in Hanover [13]. The prototype interferometer will be used to test and develop new techniques for potential future upgrades of gravitational-wave detector. The first task is to set up an all frequency quantum noise limited 10 m Michelson Interferometer see figure 3.2 [40],[39]. This interferometer is limited in sensitivity by quantum noise in a wide band around the frequency at which shot noise and radiation pressure noise are equal, the so called standard quantum limit (SQL). The light source for this experiment it an eLIGO 35 W Nd:YAG laser amplifier [10]. The coupling of the laser light into the vacuum system will be done by use of a photonic crystal fiber. The beam is then filtered by a mode filter. The laser will be stabilized to better than $2 \times 10^{-9} / \sqrt{Hz}$ in relative power noise.

Fig. 3.1 The AEI 10 m Prototype facility with $100\,m^3$ volume, 3 m diameter tanks and 1.5 m diameter beam tubes. The ultra-high vacuum system is designed in a rather generous way, such that it can hold more than one experiment at a time. The pressure inside the system is below 10^{-6} mbar after 12 hours of pumping, after one week it is below 10^{-7} mbar.
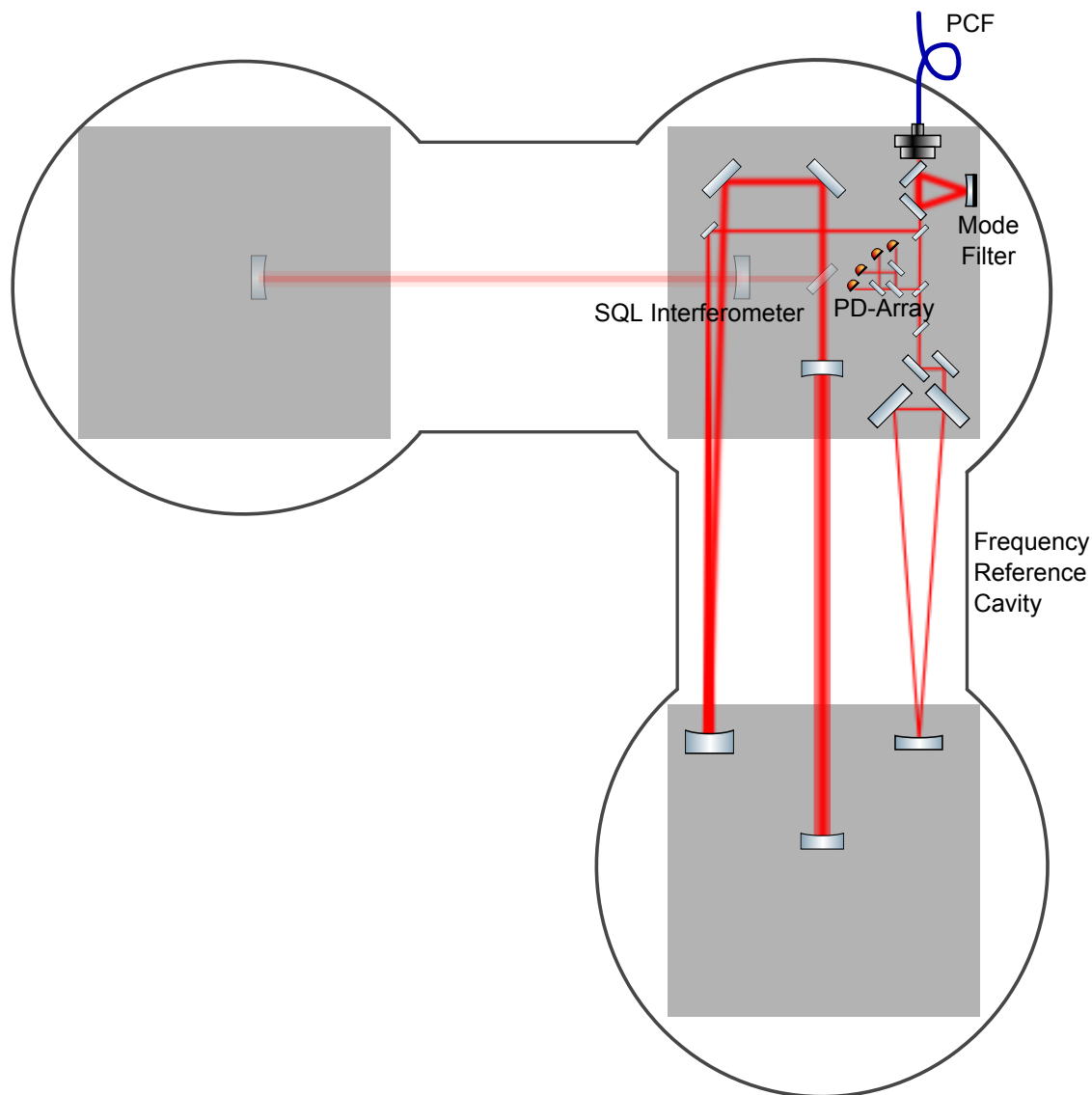
Fig. 3.2 Simplified setup of the AEI 10 m prototype. The laser light is coupled into the vacuum tank by a photonic crystal fiber. The laser light is spatially cleaned with a mode filter. For the power stabilization of the laser, a PD-Array is placed behind the mode filter.The laser frequency is stabilized to the triangular reference cavity. The main laser beam is going to the SQL interferometer.

3.1   Light source

To reach the SQL an input power of 8 W is required. Therefore a 35 W eLIGO amplifier is used as a light source. As described in chapter 2.1.1 an EOM is located in between the NPRO and the amplifier. It modulates a frequency of 35.5 MHz onto the laser light, which is later used for the stabilization of the mode filter. Additionally it is the fast actuator for the frequency stabilization of the SQL interferometer. The acousto-optic modulator is required as an actuator for the power stabilization. For this, some laser power is shifted into the first order of the acousto-optic modulator and the zero-order beam is stabilized.

3.2   Stabilization concept

Higher order modes reduce the read out sensitivity of the interferometer. To reduce the higher order mode content, a photonic crystal fiber and a mode filter are installed. The fiber differs from other optical single-mode fibers by transmitting high powers.

3.2.1   Photonic Crystal Fiber

Photonic crystal fibers are made out of one material in contrast to single mode fibers with two different materials. Optical fibers conduct the light due to the lower refractive index of the cladding compared to the core. In photonic crystal fibers, the light guiding property is generated by the micro structuring of the cladding. A microscope image of the fiber for the AEI 10 m prototype is shown in Figure 3.4 . The conductive property of the PCF depends only on diameter and spacing of the structural holes. As a result, large mode field diameters can be realized and therefore high powers can be transmitted at tolerable power densities. Additionally, the cladding structure favors the TEM00 mode of the incoming light field and thereby effects a filtering of the beam geometry. The fiber used is an LMA-PM-15 from NKT Photonics and is 4.5 m long with a massive core. The transmissive property of the fiber ranges from 750 nm to 1700 nm and the mode field diameter is 12 µm. It is a polarization maintaining fiber, because of the two stress cores. They generate a directional dependency of the refractive index. The end faces of the fiber are fused to seal it and have an angle of 8°. In order to handle the fiber during connection and disconnection, the fiber is inside of a high power SMA-905 connector.

The fiber is used to guide the laser light into the vacuum system of the AEI 10 m prototype. In contrast to a free space beam coupling trough a view port, the beam propagation
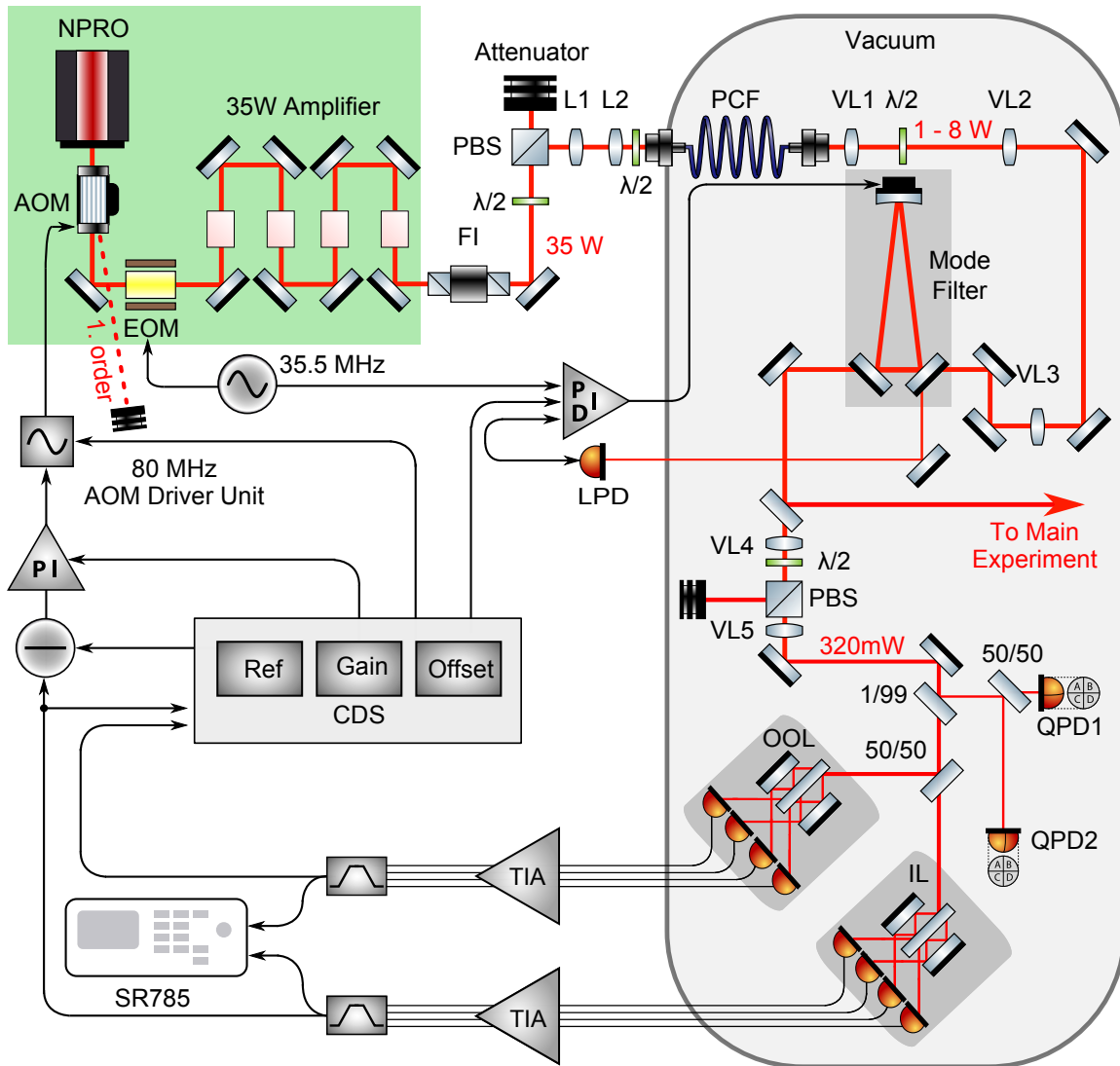
Fig. 3.3 Setup of the laser stabilization at the central tank of the AEI 10 m prototype. In the green box, the 35 W eLIGO amplifier is shown. The light is then sent through a Faraday isolator to a power attenuation unit consisting of a lambda half plate and a polarizing beam splitter. For the fiber coupling, the polarization is adjusted via a second lambda half plate. The light is transmitted by the photonic crystal fiber into the vacuum tank. The fiber out coupling, the mode filter and its mode matching telescope are located on a breadboard, mounted to the optical table. The transmitted light is split up and the main part is sent to the SQL interferometer. The remaining 320 mW are measured with four in loop photo diodes to stabilize the laser power and four out of loop photo diodes observed the achieved power stability.
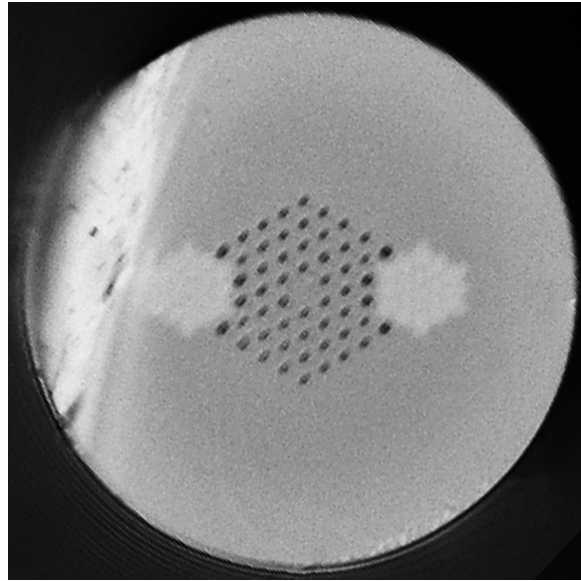
Fig. 3.4 Profile of the polarization maintaining photonic crystal fiber. The light remains trapped in the core due to a micro structured cladding. Two stress cores generate a directional dependence of the refractive index and thus preserve the polarization.

after the fiber is independent of relative movements between the laser system and the isolated optical tables inside the vacuum system of the prototype. The components of the fiber coupling as well as the 35 W amplifier are located on an optical table next to the central vacuum tank of the AEI 10 m prototype. The layout of the fiber coupling is shown in figure 3.3. The light passes through a Faraday isolator of the IO-5-1064-HP model from Thorlabs with a transmission of 93 %. The laser light is attenuated by a half-wave plate and polarization beam splitter.

The fiber core diameter is 15 μm and therefore the mode field diameter must be 12 μm [4]. In order to adapt the laser beam to the mode of the PCF, two lenses are used. A lambda half-plate is used to adjust the polarization to the fiber axis. A coupling efficiency of over 75 % could be reached. By design, the non-transmitted light is scattered diffusely out of the fiber cladding. Therefore, recesses are cut into the high power fiber connector. The maximum transmitted power was 20 W and no effects of stimulated Brillouin scattering could be found.

3.2.2 Triangular Mode Filter Cavity

To suppress fluctuations of the beam position and angle, a mode filter is used. These fluctuations can be descried as higher order mode contaminations. A detailed description
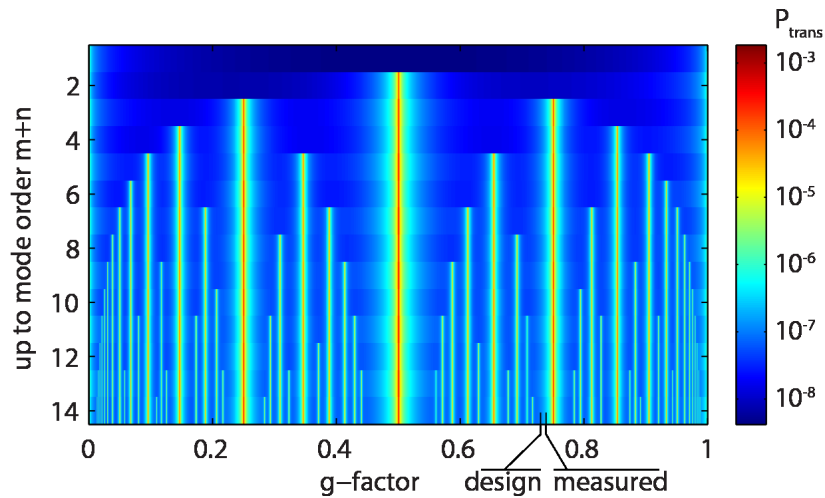
Fig. 3.5 Transmission of higher order modes through the triangular mode filter with varying g-factor is shown.[3]

can be found in [20]. To suppress the higher order mode content a triangular optical cavity which favors the TEM00 mode was developed [3]. A mode filter transmits the laser power as a function of the beam geometry. The fundamental mode and the quantitative suppression of the higher modes is determined by the optical parameters of the resonator. The curvatures of the mirrors and the wavelength of the light field, determine the fundamental mode of the resonator, which is quantized by the g-factor [3]. The suppression of the higher order modes is determined by the finesse, the circulating losses and the g-factor of the resonator. The mode filter consists of three mirrors and forms an isosceles triangle with the circulating light. A 3d drawing of the mode filter is shown in figure 3.6. The mode filter consists of two planar and one curved mirror. The planar mirrors serve for coupling in and out of the laser light. The curved mirror is located on the symmetry axis of the triangle and creates a stable resonator. The reflectivity of the mirrors determines the finesse of the resonator. The finesse scales linearly with the suppression of the field amplitude of the higher order modes. As displayed in figure 3.5 a good suppression is achieved with a g-factor of 0.735 [3]. Especially modes with a low order are not resonant at this g-factor. In addition, this is a relatively large distance to the contributions of the first and second order. The radius of curvature for the curved mirror is 1 m. This results in a circular length of 53 cm and a beam radius of 386 µm between the two planar mirrors. The optical design parameters of the mode filter are summarized in table 3.1.

To achieve a ridged assembly of the mirrors, a metal spacer is used. The geometry of the resonator defines the positions and tilting angles of the mirrors. A sectional view of the mode filter is shown in Figure 3.6. The distance between the two planar mirrors
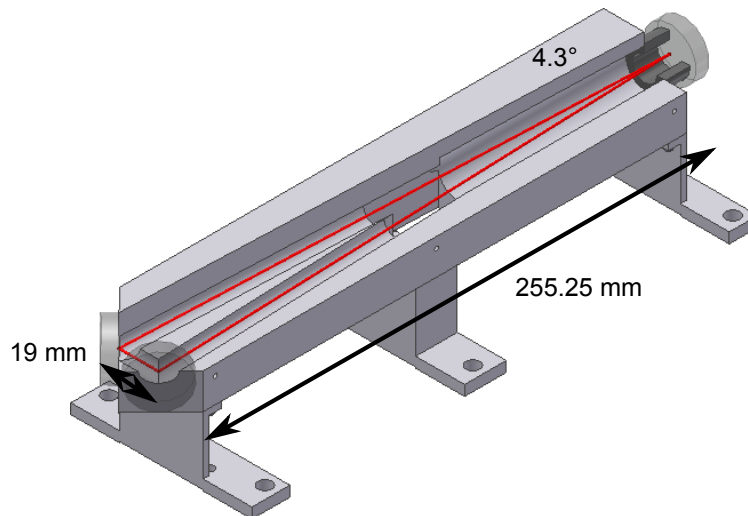
Fig. 3.6 3D CAD drawing of the mode filter and the mounting structure. The beam path is shown in red. The two planar mirrors are separated by 19 mm and the curved mirror is at a distance of 255.25 mm. The angle between the two plane mirrors is 4.3°.

is 19 mm and the distance to the curved mirror is 255.25 mm. This results in a reflection angle of 2.15°. The spacer is made out of Super Invar, because of its extremely low thermal expansion coefficient. The two planar mirrors are for coupling in and out of the cavity and have a reflection of 99.67 % for vertically polarized light. The third concave mirror is highly reflective with a reflection coefficient of 99.998 % and has a radius of curvature of 1 m and is designed for an angle of incidence of 0°. In order to be able to adapt the resonator length to the frequency of the laser light, a piezo is located between the spacer and the curved mirror. The vacuum-compatible NAC2125-H12-C01 from Noliac is 12 mm thick and has a stroke of 13.3 μm with an operating voltage of −40 V to 200 V.

The mode filter and its mode matching lenses were assembled on a dedicated bread-board before they were installation inside the vacuum system of the AEI 10 m prototype. It is located in the north-east corner of the central isolated optical table. The final assembly is shown in picture 3.7. The light passes from the photonic crystal fiber through the collimating output lens with a focal length of 6.24 mm. Two super polished and anti reflective coated lenses and adapt the beam to the mode filter. The second lens, with a focal length of 400 mm, is located at a distance of 10 cm and the third lens, with a focal length of 300 mm, at a distance of 55 cm from the fiber output.
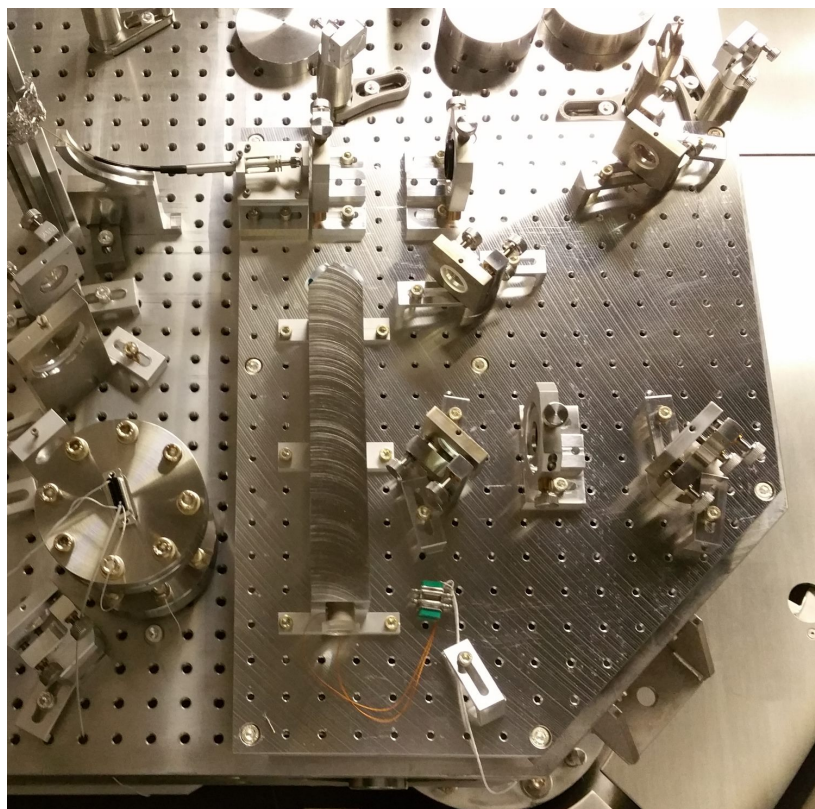
Fig. 3.7 Photo from the top of the mode filter breadboard. On the left upper side is the photonic crystal fiber coming from one of the upper flanges. After decoupling and collimating the beam with a 6.24 mm lens, the light is sent to the mode filter via two additional lenses. L2 with a focal length of 400 mm and L3 with 300 mm . Both are super polished to avoid stray light. To adjust the incoming beam to the mode filter, two mirrors are placed in front of it.

Electronics and stabilization

The stabilization of the mode filter is done with a feed back system. A deviation of the resonator's resonance frequency from the laser frequency is detected by a photo diode and stabilized with the Pound-Drever-Hall method [5]. This control difference is then converted by the controller of an external electronic into a control variable which is converted by the piezo into a length deviation of the resonator. For this purpose, the power reflected at the resonator is measured with a locking photo diode (LPD), see figure 3.3. With a deviation of the resonator length, the light is no longer in resonance and the reflected power increases. Due to the symmetry of the resonance, this signal lacks information about the direction of the length deviation. Therefore sidebands are imprinted onto the incoming laser beam. These are reflected at the in coupling mirror, when the cavity is resonant for the main beam. The phase measurement of the main beam, relative to the sidebands, creates an asymmetric error signal. An aLIGO PSL locking photo diode is used to detect the reflected light, a schematic diagram can be found in the appendix. The servo electronics are also based on a model from aLIGO. In addition to the analog stabilization, a digital control of the stabilization is integrated into the CDS of the AEI 10 m prototype [7]. It also includes an auto lock procedure.

Characterization

In order to characterize the mode filtering effect of the cavity and the photonic crystal fiber, a series of measurements were performed and analyzed. All measurements were made after the mode filter was installed in the vacuum system. In order to evaluate the similarity between the fiber mode and a fundamental Gaussian mode, transmitted by the photonic crystal fiber, and to determine the finesse of the resonator, a mode scan was analyzed [3]. In figure 3.8 a scan over one FSR and the higher order modes are shown. The open loop transfer function of the feedback control is used to characterize the stabilization. In order to analyze the light behind the mode filter, the relative power noise and the frequency noise were measured.

To adjust the servo to the mode filter, the error signal was optimized for the mixer. For this purpose, the photo diode signal is mixed with the local oscillator signal in the mixer electronics. The phase of the local oscillator signal it matched to the phase of the photo diode signal, when having symmetrical side band signals. The sidebands are spaced from the fundamental mode at the distance of the modulation frequency. In the mode filter this is 35.5 MHz.
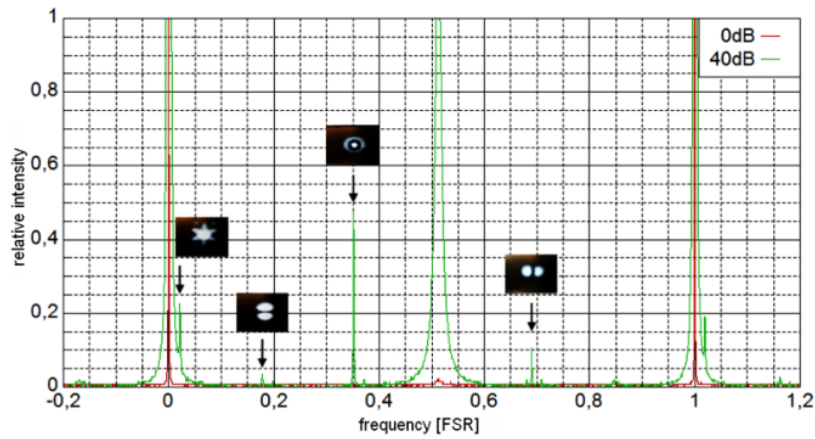
Fig. 3.8 Mode scan measured with the mode filter cavity. The peak in the center is due to the residual horizontal polarization [3]. Measured with two amplifications of the photo detector.
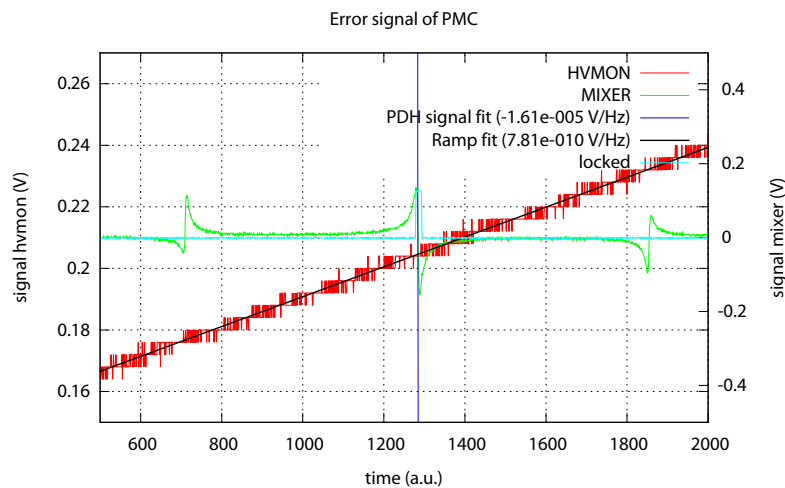
Fig. 3.9 Error signal of the mode filter plotted over time. The MIXER signal of the servo in Green with the fundamental mode is shown in the center and the sideband of the Pound-Drever Hall signal is offset by 35.5 MHz. In addition the HV-MON is marked in red.
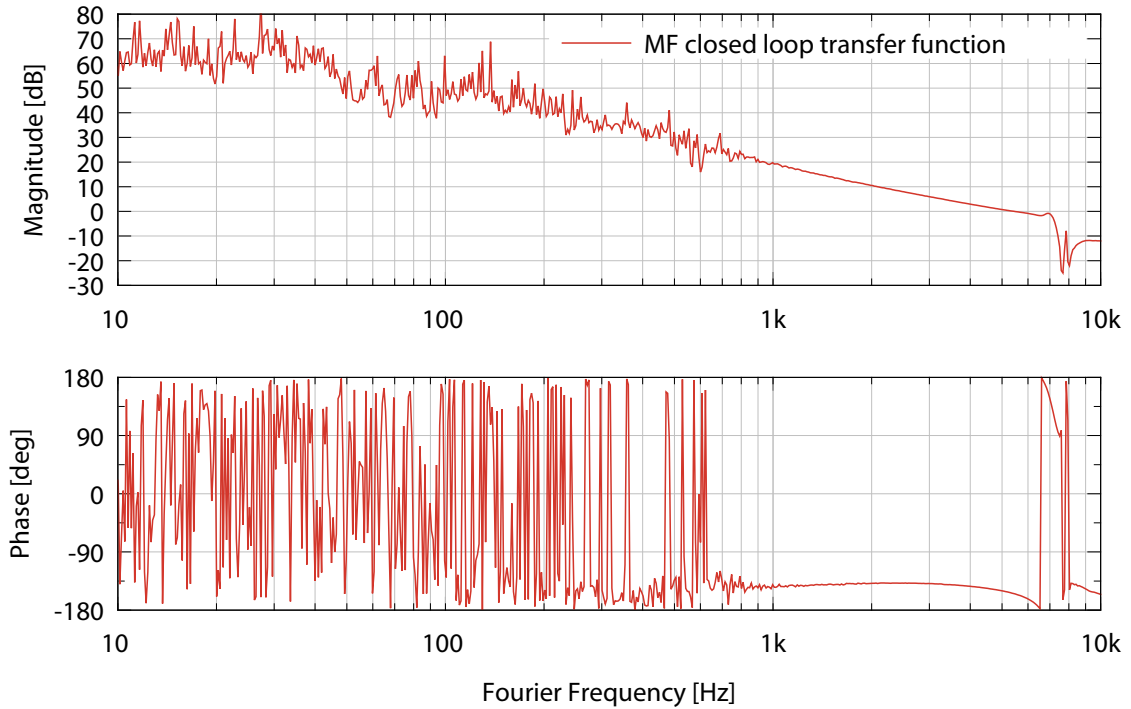
Fig. 3.10 Closed loop transfer function of the mode filter length stabilization, with the unity gain frequency of 5.3 kHz and a maximum suppression of 60 dB at 10 Hz. In the measurement band of the interferometer, at 200 Hz, there is 45 dB suppression.

In order to characterize the control loop of the stabilization, the transfer function of the closed control loop was measured. It was measured by a network analyzer, with a swept sine of an amplitude of 10mV. The amplitude and phase behavior of the control loop in the range from 10 Hz to 10 kHz is shown in Figure 3.10. With a unity gain frequency of 5.3 kHz and a maximum suppression of 60 dB at 10 Hz. In the measurement band of the SQL Interferometer, at 200 Hz, there is 45 dB suppression. The piezo actuator has a slope of $44\,\mathrm{nm\,V^{-1}}$ at a voltage offset of 100 V.

The relative power noise of the light was measured by a photo diode in transmission of the cavity and was analyzed with a spectrum analyzer. The light behind the mode filter had an output of 8 W and was attenuated by a mirror with a transmission rate of 1 %. The relative power noise of the light between 10 Hz and 100 kHz is shown in Figure 3.11. It is $4 \times 10^{-5}\,/\sqrt{\mathrm{Hz}}$ at 10 Hz and $3 \times 10^{-7}\,/\sqrt{\mathrm{Hz}}$ at 100 kHz.

The frequency noise of the laser is measured with the help of the mode filter by measuring its length deviation. The mode filter is quieter in length noise than the 35 W eLIGO amplifier in frequency noise. The measurement is split into two signal paths. At low frequencies, it is the control signal of the mode filter piezo actuator, at high frequencies,
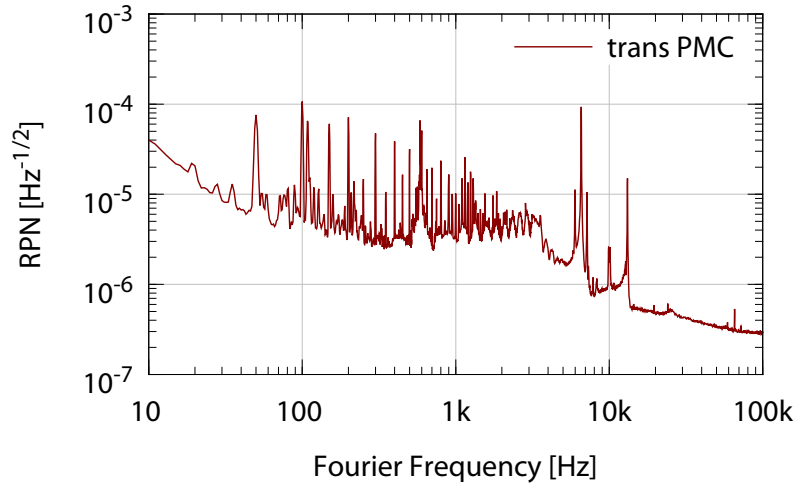
Fig. 3.11 Relative power of the 35 W eLIGO amplifier guided through the photonic crystal fiber and the mode filter. The resonance at 50 Hz and its harmonics are due to a grounding issue.

the error signal. The projected noise of a NPRO is plotted as a reference. In figure 3.12 it can be seen that the measurement of the noise exactly follows the projected NPRO measurement. There is a resonance at 600 Hz of the spacer body and the piezo resonance at 5.3 kHz.

3.2.3 Power stabilization

All classical noise sources must be suppressed below the standard quantum limit at the AEI 10 m prototype. This also includes the relative power noise which should be attenuated in the experiment down to $2 \times 10^{-9} / \sqrt{Hz}$ [16].

A photo diode array had been developed at AEI to reach such stabilities at the aLIGO detectors[25]. A newer iteration of this Array [18], which was built at LIGO, was adapted and installed at the AEI 10 m prototype. Besides changing the height of the photo diode array, according to the beam height within the prototype, our adaption included strain reliefs as well as a second QPD to ensure for perfect alignment. In addition, the electronics were reworked and equipped with low-noise trans impedance resistors as well as additional diagnostic signals.
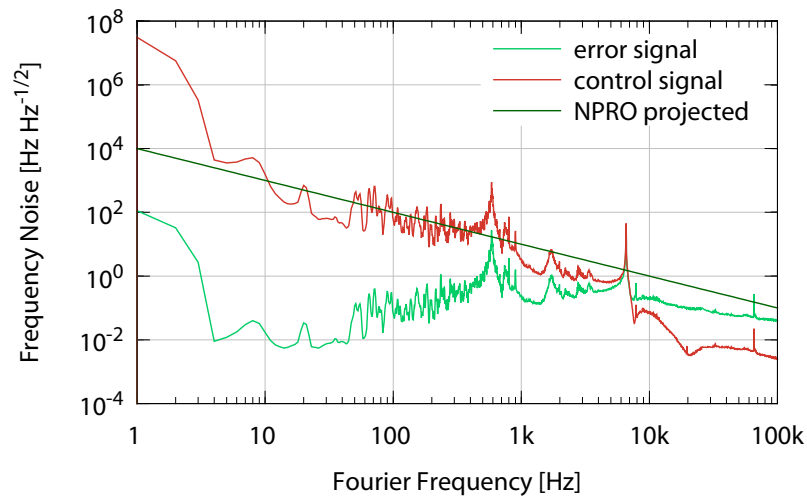
Fig. 3.12 Measurement of the frequency noise of the laser measured with the length of the mode filter. The measurement is split into two sections. The error signal and the control signal. They cross at 5.3 kHz and the resonance of the piezo is visible.

Optical Setup

A detailed overview of the feedback control loop can be found in figure 3.3.

The acousto-optic modulator (AOM) [Crystal Technology Inc., AOMO 3080] of the 35 W eLIGO amplifier serves as actuator and the photo diode array inside of the vacuum system is used as sensor. It is located behind the NPRO but before the amplifier unit. 320 mW were detected by the photo diode array for power stabilization. The first design of the photo diode array was developed in the AEI and consisted of eight InGaAs photo diodes [Perkin Elmer,C30642] with an active diameter of 2 mm and an average responsivity of about 0.79 A W^{-1} [25]. They are individually movable by 1 mm in transversal direction. A attenuation unit ensures that the power sent to the photo diode array can be adjusted. In the housing of the photo diode array 1 % of the light is split of and send to the two quadrant photo diodes [OSI Optolectronics, Q3000]. The QPDs have an active diameter of 3 mm and a gap of 45 μm. In addition to the single QPD design of LIGO, a second photo diode was installed for the beam alignment to the PD array in a unaccessible area like inside a vacuum tank. The beam radius on QPD1 is 250 μm and on QPD2 it is 100 μm, with a Gouy phase difference of 90° between the two detection points. With this Gouy phase difference the modified photo diode array provides information on all alignment degrees of freedom of the laser beam with respect to the photo diodes and hence for remote alignment. The remaining light of about 310 mW is then split up into half and send to the two photo diode planes. As displayed in figure 3.13, both planes consist of
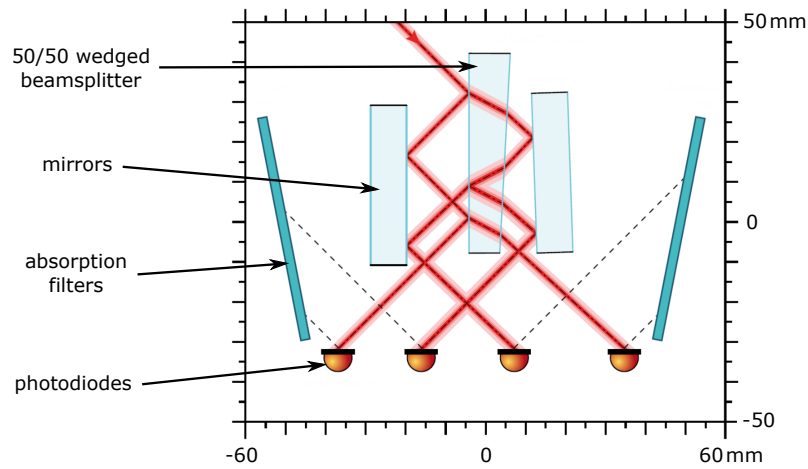
Fig. 3.13 Beam path on one level of the photo diode array with the monolithic beam separation.

an angled beam splitter and two highly reflective mirrors. The photo diodes are set at an angle of 45° so that the reflected beam can not influence with the measurement. Each detect a power of 37.5 mW to 44.5 mW. All non-absorbed light is absorbed in BG39 filters which is hit under the Brewster angle. The beam diameter on all eight photo diodes is between 170 μm and 330 μm.

Electronics

All eight single element photo diodes and the two QPD are connected with a vacuum-compatible cable which are routed to the outside. The readout electronics consists of a filtered bias voltage and the trans impedance amplifier (TIA). The eight voltages of the TIA were band-passed to increase signals between 3 Hz and 2.5 kHz by 34 dB. An additional high pass reduces the signal at low frequencies by 20 dB. This is done to prevent saturation effects.

The signals of the four upper photo diodes and respectively the four lower photo diodes are added up and used as in loop/out of loop signals for the control loop to stabilize the laser power. With the sum of the other four signals the achieved stability could be verified. The CDS installed in the AEI 10 m prototype is used for the control of the system. The in loop sum signal was subtracted from a low-noise low-pass filtered voltage reference provided by the CDS. The analog electronics of the servo include two optional integrators and a variable gain stage. This is forming a proportional-integral controller. The error signal is amplified by the loop gain by more than 90 dB at frequencies below 200 Hz. To
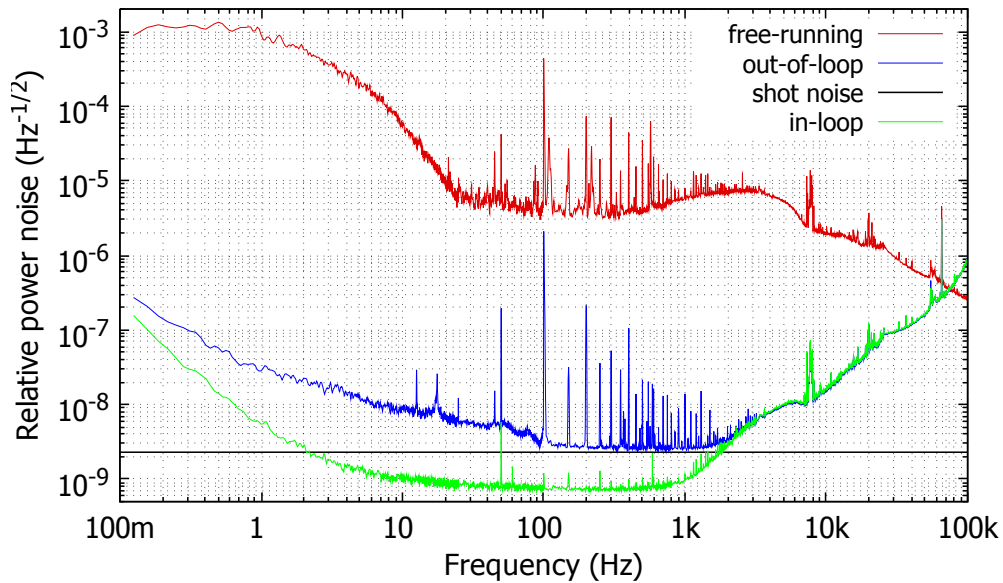
Fig. 3.14 Performance of the power stabilization. Relative power noise measured by the in loop and the out of loop photo detectors in comparison to the free-running laser. The black shot noise limit has a value of $2.29 \times 10^{-9} / \sqrt{Hz}$ [35] and was calculated by taking the photo currents of all four photo diode in loop with 115.5 mA and out of loop 128.8 mA.

control the amplitude of the laser beam, a fraction is taped off with an AOM and dumped. The AOM is modulated with a frequency of 80 MHz for the first diffraction order. The operating point for the stabilization is at an offset of 5 % for the deflected light.

Shot-noise-limited laser power stabilization

The free-running noise was measured by the photo diode array to determine the gain.

Then, the servo has been adjusted so that the loop gain is suppressing the in-loop signal below the shot noise [35]. The out of loop signal is limited by shot noise between 100 Hz to 1 kHz . The measured free-running RPN is $4 \times 10^{-6} / \sqrt{Hz}$ in the frequency region around 200 Hz. With the closed feedback control loop it was possible to detected an out of loop RPN of $2.6 \times 10^{-9} / \sqrt{Hz}$ for frequencies from 100 Hz to 1 kHz. The total powers measured on the two sensors were out of loop 163 mW and in loop 146 mW resulting in a relative shot noise level of $2.29 \times 10^{-9} / \sqrt{Hz}$.

Furthermore, no performance differences were observed by interchanging the photo diodes of the in and out of loop path. With this knowledge, we deduced a 3 dB lower RPN of the laser beam in the out of loop path. At 200 Hz this calculated value is $1.84 \times 10^{-9} / \sqrt{Hz}$. The unity gain frequency was estimated to be 140 kHz. The system is long term stable and

was running several days. At frequencies greater than 75 kHz, the in loop and out of loop graphs crossed the free-running measurement and are followed by noise amplification due to low phase margin, at about 160 kHz not shown in figure 3.14. The main reason for the excess noise at low frequencies is probably created by beam pointing and scattered light. Each one of the eight photo diodes are attached to a cone-shaped aluminum case. With an IR-viewer scattering of light at these cones was observed and could be one of the scattered light sources. Under vacuum, a constant pointing fluctuation of at least 1 µm was observed with the QPD. Finally, the RPN of the out of loop measurement showed sharp line harmonics of the power grid frequency of 50 Hz dominating the spectrum. This effect was assumed to result from ground loops between several electric components in the environment of the AEI 10 m Prototype and was not analyzed further.

3.3   Summary

Within this thesis a 35 W eLIGO amplifier was set up for the AEI 10 m Prototype interferometer. Pointing reduction and pure fundamental beam shape was crucial for the interferometer. To avoid initial pointing and as initial filter for the spatial mode profile, a photonic crystal fiber was installed and used to coupe up to 8 W of laser power to the inside of the vacuum system. For additional filtering a triangular spacer cavity is used as a mode filter directly behind the fiber out coupler.

Furthermore the aLIGO PD Array design was improved with an additional QPD. This allowed to prealign th PD Array out of the vacuum and find the correct alignment after installation in the vacuum system. The PD Array was successfully installed within the AEI 10 m Prototype vacuum system, aligned and used to stabilize the laser beam to reach the $2 \times 10^{-9} / \sqrt{\text{Hz}}$ in relative power noise. It also serves as a testbed, to ease the implementation and the long therm use at LIGO.

35 W Laser System	
output power	35 W
frequency	1064 nm
power in ground mode (TEM00)	95 %
Photonic Crystal Fiber	
length	4.5 m
mode diameter	12 μm
transmission	75 %
Mode Filter	
g-factor	0.735
ROC of the HR mirror	1 m
round trip length	53 cm
waist	386 μm
R of planar mirrors	99.67 %
free spectral range	566 MHz
line width	604 kHz
finesse	937
transmission	95 %
Stabilization	
modulation frequency	35.5 MHz
modulation depth	1.5 mrad
unity gain frequency	6 kHz

Table 3.1 Comprehensive data of the PCF and the mode filter.

Chapter 4

70 W Amplifier for aLIGO

The aLIGO high power oscillator is a complex and difficult to maintain laser system. Currently it is the only laser system delivering 200 W of output power with excellent beam parameters. At the LIGO Livingston observatory a failure of the high power oscillator happened. Until the high power oscillator is running again, a intermediate solution for the upcoming observation runs had to be found. In this chapter, two different solid state amplifiers are analyzed. The first is a possible laser amplifier for aLIGO, amplifying up to 70 W and it is described in section 4.2. A second one, described in section 4.3, is used for weak seed sources, amplifying up to 8 W. For characterization, the diagnostic breadboard was used and is described in section 4.1.

4.1   Diagnostic Breadboard

The Diagnostic Breadboard (DBB) was developed in the AEI for a detailed laser beam analysis [22, 23]. The power noise, frequency noise, beam pointing fluctuations and spatial beam quality can be measured automatically in a Fourier frequency band from 1 Hz to 100 kHz. Additionally power noise can be measured by a spectrum analyzer up to 100 MHz. The DBB was designed for characterization of linearly polarized, single-frequency, continuous wave laser beams at a wavelength of 1064 nm and was optimized for an input power of 135 mW. The optical layout of th DBB is shown in figure 4.1.

The power of the input beam and the power fluctuations were measured with the photo detector RPD. A photo current of 50 mA can be detected with a bandwidth of 45 MHz. This results in a shot noise limited sensitivity of $2.5 \times 10^{-9} / \sqrt{\text{Hz}}$.

Frequency fluctuations of the input beam were measured with the optical ring resonator. It has a finesse of 356 and a FSR of 715 MHz. The round-trip length of 420 mm can be varied by 5 μm with a piezo which is attached in between the spacer and the curved mirror of the resonator. The resonator is stabilized to the frequency of the input beam using a dither lock with a modulation frequency of 1 MHz. Frequency fluctuations of the input beam are composed from the control and error signal in a Fourier frequency band from 1 Hz to 100 kHz.

The pointing fluctuations of the input beam is measured by using the differential wavefront sensing (DWS) and the ring resonator as the pointing reference [27]. Pointing deviations between the fundamental mode, to which the resonator was stabilized, and the input beam are measured. Two quadrant photo detectors, QPD1 and QPD2, were used to detect the DWS signals. In order to stay within the linear range of the DWS signals, the pointing of the input beam was adjusted in servo loops using two mirrors PZT1 and PZT2 that could be tilted with piezos.

The spatial beam quality of the input beam was measured with a length scan of the resonator. The resonator round-trip length was modulated with a ramp signal by several micro meters, with a modulation frequency of 10 Hz. The transmitted power was measured with the photo detector TPD. The high order mode content is the sum of the power of the higher order modes, transmitted through the resonator.

4.2   neoVAN - 70 W solid state amplifier

The neoLASE neoVAN is a further development of the four-stage amplifier of the eLIGO 35 W amplifier [29]. It consists of four Nd:YVO crystals and is pumped by four laser diodes via fibers. The pump light has a wavelength of 808 nm. A picture is shown in figure 4.2. A compact solid state amplifier was analyzed and can now be implemented into the existing table layout at the detectors. It provides 70 W of output power, when the 35 W amplifier is used as a seed.

This amplifier will ensure that enough laser power will be available to start the next science/observation runs with the anticipated input power. Our Implementation will offer the possibility to choose freely between three configurations, the 35 W amplifier, the 70 W amplifier and the HPO with 200 W output power ones repaired.
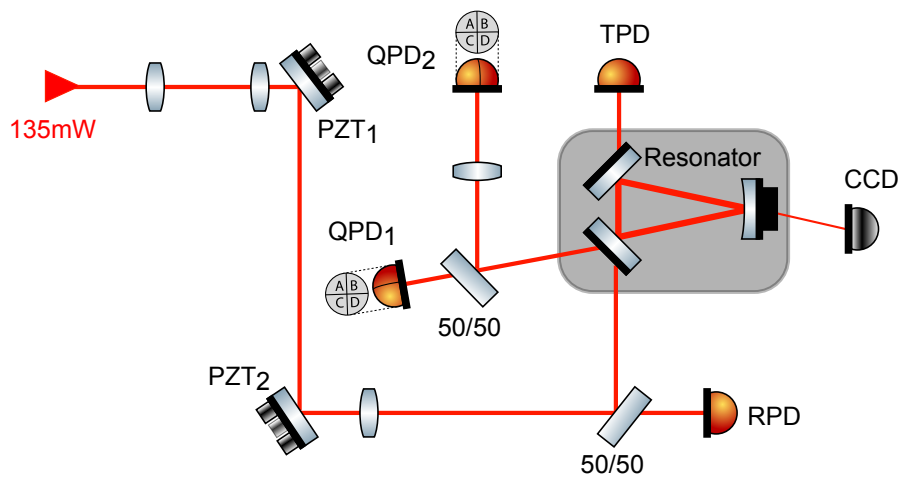
Fig. 4.1 The schematic composition of the diagnostic breadboard. The main component is the three-mirror resonator with a curved mirror which can vary the length of the resonator through a piezo. This is used to measure the intrinsic mode of the incoming beam in combination with the transmission TPD. To ease the adjustment of the incoming beam, to the eigenmode of the resonator, a CCD in transmission is set up. The RPD photo diode is used to determine the relative power noise. To measure the frequency noise, the resonator is stabilized with a piezo onto the laser light. For pointing measurements, two piezo for x and y actuation and two quadrant photo diodes are installed, with a Gouy phase separation of 90°.
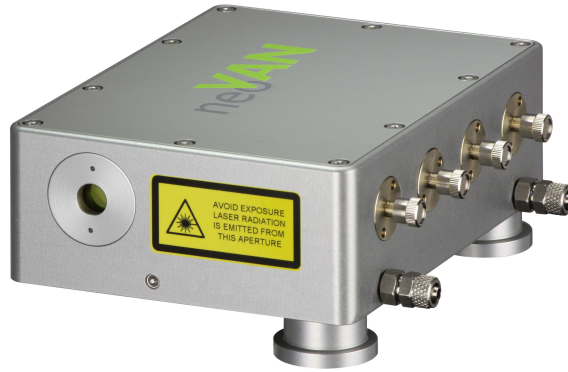
Fig. 4.2 Picture neoVAN of the company NEOLASE which is used in the 70W amplifier system. With four crystals pumped with four fiber coupled diodes.

First, the amplifier was tested and characterized in the AEI together with 35 W amplifier of the engineering prototype (EPT). It was then integrated into the aLIGO reference system to test the possible implementation into the LIGO observatory.

4.2.1   Experiment at EPT 35 W Amplifier

The first test of the new amplifier was done by using the engineering prototype 35 W amplifier. The optical table was equipped with a DBB to characterize the new amplifier. With this, it is possible to seed the 70 W amplifier with the full 35 W and measure all important beam characteristics. Four fibers are connected to the amplifier, each with 45 W pump diode at a wavelength of 808 nm. Via two alignment mirrors the light is fed into the amplifier. A schematic diagram of the system is shown in figure 4.3. To attenuate the light for the measurements a mirror with 1 % transmission rate was installed behind the 35 W amplifier and behind the 70 W amplifier. The maximum achieved power was 80 W, with a higher order mode content of 8 %.

Relative power noise

In order to be able to compare the relative power noise of the 70 W amplifier, the noise of the 35 W eLIGO amplifier was measured first. This measurement is shown in green in figure 4.4. The measurement performed with the 70 W amplifier is shown in dark blue. As the diode driver a LDP-CW series made by PicoLAS was used. It has a wide noise between 500 Hz and 10 kHz as well as peaks of the switching frequencies at 20, 40, 60 and 80 kHz. To reduce this noise, the initial current drive was replaced by the same model used at the
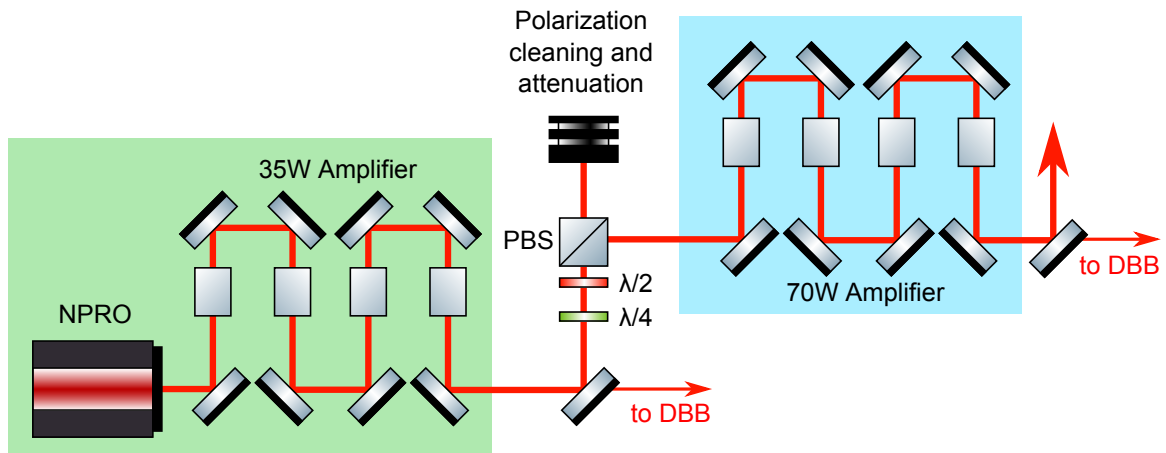
Fig. 4.3 Simplified design of the 70 W amplifier. As a seed the 35 W eLIGO amplifier was used and its light was sent through a variable power stage to the 70 W amplifier. Later the system was installed in the aLIGO reference system and its 35 W amplifier was used as the seed.

35 W amplifier, made by Lumina. Afterwards the power noise was measured again (dark red curve). Here it can be seen that the switching frequencies are significantly smaller but the broadband noise is still there. Two capacitors by KEMET with a capacity of 1500 µF were installed between the laser diode and the current driver to form a low pass. These tests were made for both drivers and are drawn in light blue and red. The best result were achieved with the current drivers of Lumina and the capacitors. For lack of space however, the combination of the Pico drivers and capacitors were used in the following measurements. Thus all subsequent measurements used this combination.

Frequency noise

The frequency noise of the new amplifier is compared to the approximated NPRO noise and the 35 W amplifier in figure 4.5. For this, the noise of a 2 W NPRO is projected. The measurement for the 35 W amplifier is plotted in green, which follows the NPRO noise over the entire frequency range. The measurement of the 70 W amplifier is shown in red and stays close to the NPRO noise as well. At frequencies between 10 Hz and 100 Hz it is a factor of two more noisy and in the range between 1 kHz and 10 kHz it does not fall under the projection like the 35 W amplifier. The amplifier is not significantly introducing additional frequency noise.
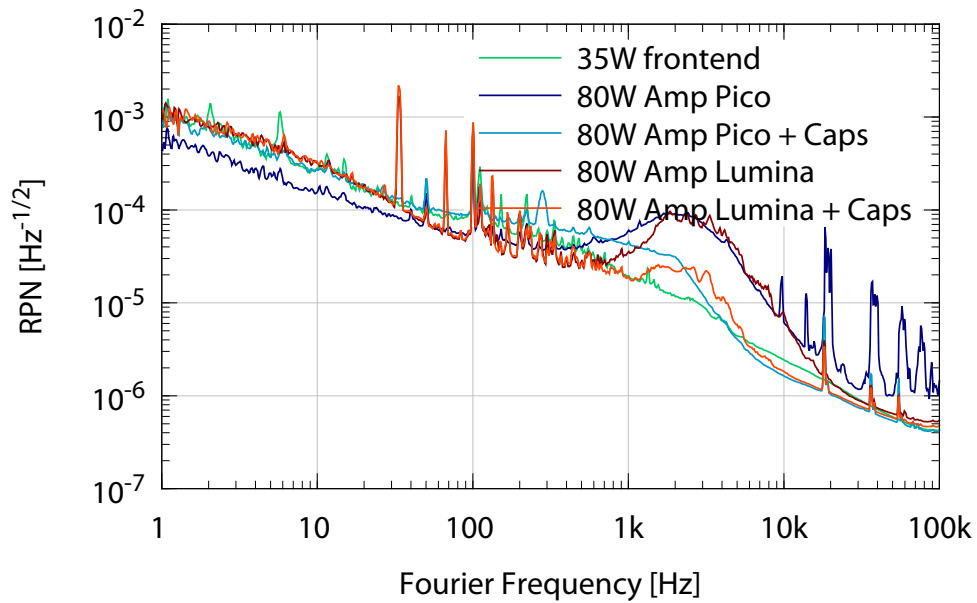
Fig. 4.4 Relative power noise measurements for the 70 W amplifier. As a reference, the 35 W amplifier is shown in red. Two different types of diode current drivers were tested for the pump diodes of the 70 W amplifier. The switching frequencies between 20 kHz and 100 kHz, can be low pass filtered with additional capacitors (Caps). The two diode drivers without the capacitors have a significantly higher noise from 1 kHz to 10 kHz. The driver of PicoLAS., additionally, shows higher switching frequencies between 20 kHz and 100 kHz. By using the capacitors, both current drivers have a lower noise which almost reaches the noise of the 35 W amplifier. The switching frequencies also become significantly smaller.
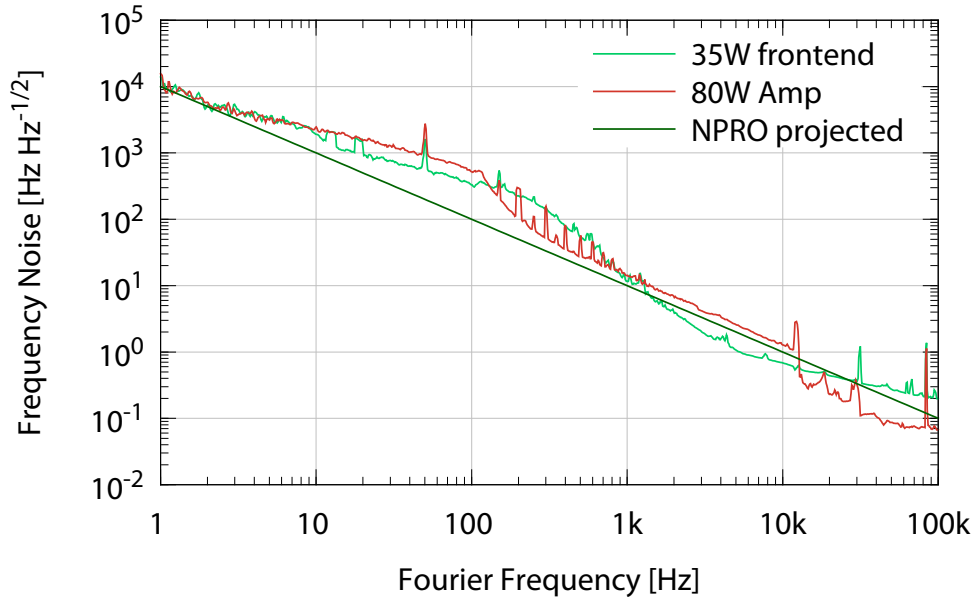
Fig. 4.5 Frequency noise of the 35 W amplifier and the 70 W amplifier. The projected frequency noise of the NPRO lasers is applied as a reference. The 35 W amplifier frequency noise is following the projected NPRO noise. The 70 W amplifier shows a similar behavior and is not introducing frequency noise. The variations are well inside the expected measurement range.

4.2.2   Implementation in the aLIGO Reference System

Since the 70 W amplifier characterization showed a sufficient performance, the implementation, the integration into the aLIGO reference system, at the AEI, could be started. The possibility, to choose between, the 35 W amplifier, the 70 W amplifier and the high power oscillator with 200 W, as input to the interferometer, was realized. Additionally an independent measurement of each stage can be performed with the DBB.

Table layout

The complete design of the amplifier is shown in Figure A.3. The basic idea was to leave the high power oscillator path as unaffected as possible. This means that only one mirror before the HPO was exchanged for a combination of lambda half plate and polarization beam splitter. Thus, the power of the 35 W amplifier can be arbitrarily divided between HPO and the new 70 W amplifier. Otherwise no change was made to the HPO. The existing optics which are usually used for the DBB path of the 35 W amplifier are reused to adjust the laser into the new amplifier. As protection against reflections for the 35 W amplifier,
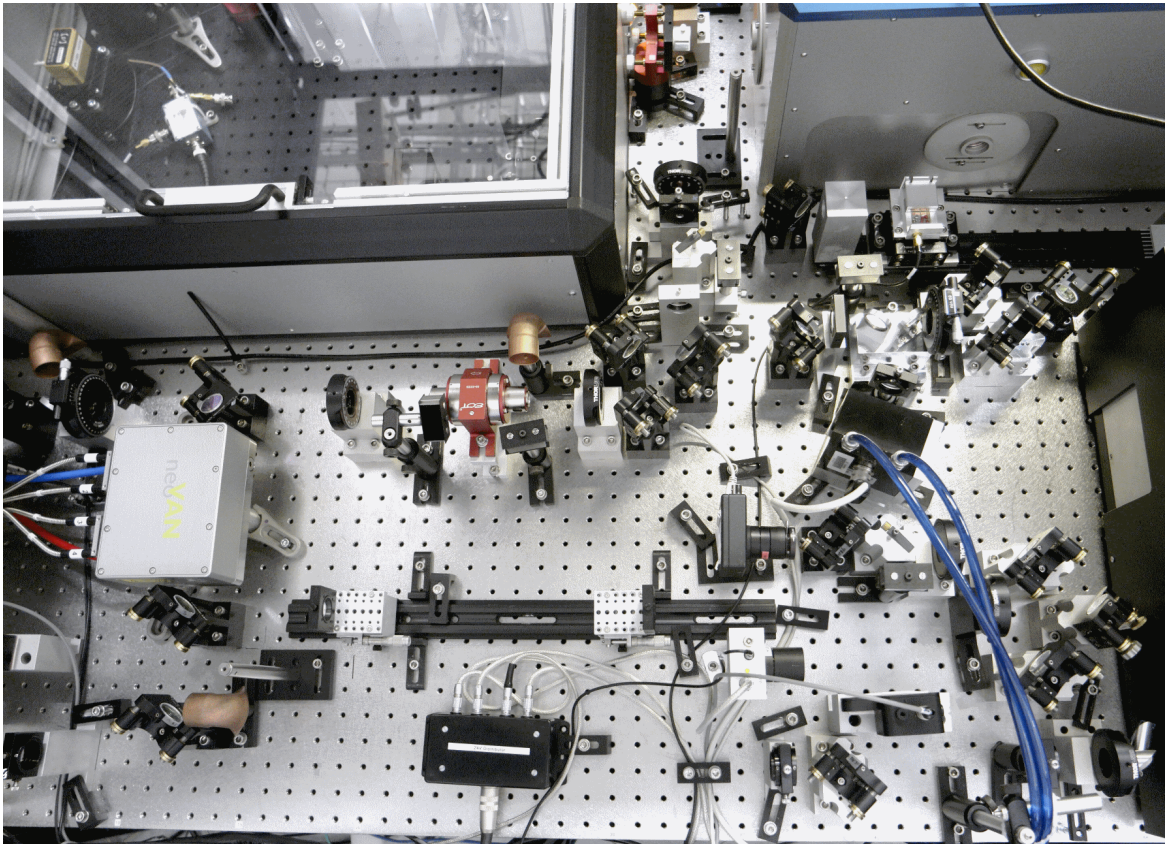
Fig. 4.6 Image of the 70 W amplifier, installed inside the reference system.

an additional Faraday Isolators from Newport was installed (ISO-FRDY-08-1064-N). The amplified light of the 70 W amplifier is then directed into the HPO laser beam via four adjustment mirrors and two mode matching lenses. The original DBB path of the HPO can be used to characterize the 70 W amplifier. To obtained the measurements from the 35 W amplifier with the DBB, the mirror before the 70 W amplifier is 1 % transmissive. A picture of the final integration of 70 W amplifier in the reference system is shown in 4.6.

After the new amplifier was installed, the pump power was carefully increased, while monitoring the beam profile with a Wincam. The power was increased until the first saturation effect on the beam profile developed. The Gaussian intensity distribution is not equally amplified anymore. At the maximal intensity of the seed beam most pump photons are already converted and the seed can not be amplified furthermore. At the edge of the beam the amplification is still possible and therefore the beam shape is deformed. With the maximum seed power of 35 W, an output power of 72 W could be achieved. The higher order mode content was 8 %.
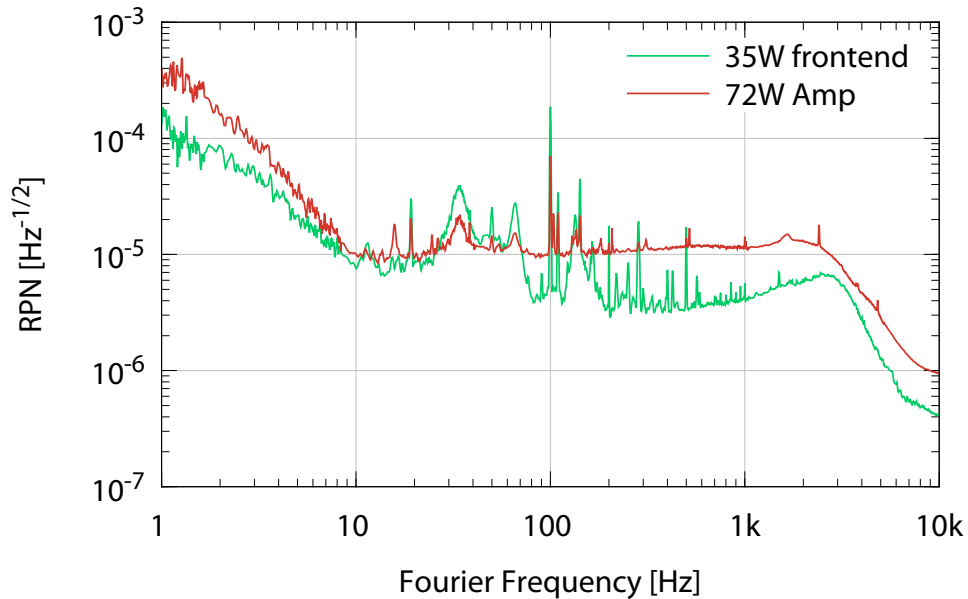
Fig. 4.7 Power noise of the 35 W amplifier of the reference system and the 70 W amplifier. Whereby the 70 W amplifier rushes over the entire frequency range by a factor of two to three more. At 1 Hz it increases from $2 \times 10^{-4}\,/\sqrt{\text{Hz}}$ to $4 \times 10^{-4}\,/\sqrt{\text{Hz}}$ and in the range between 10 Hz and 3 kHz the noise is broadband flat at $1 \times 10^{-5}\,/\sqrt{\text{Hz}}$, then falls on the $1 \times 10^{-6}\,/\sqrt{\text{Hz}}$ at 10 kHz.

Relative power noise

Since the 35 W amplifiers of reference system has a better noise performance than the 35 W amplifier used in section 4.2.1, the measurement were repeated. The relative power noise was measured after the installation at the reference system. In figure 4.7, the 35 W amplifier is shown in green, and the 70 W amplifier in red.

The 70 W amplifier has a higher relative power noise compared to the 35 W amplifier. A broadband increased noise level from 100 Hz to 2 kHz and increase to low frequencies are visible. However, the noise is better than the noise of the high power oscillator.

Frequency noise

The frequency noise was also measured for the 35 W amplifier and for the 70 W amplifier. The results are shown in figure 4.8. Both measurements are split into error and control signals. The 35 W amplifier is shown in green and the 70 W amplifier in red. It can be seen that the control signal dominates at low frequencies and both measurements are identical and follow the NPRO noise. From about 1 kHz the control signal dominates and indicates
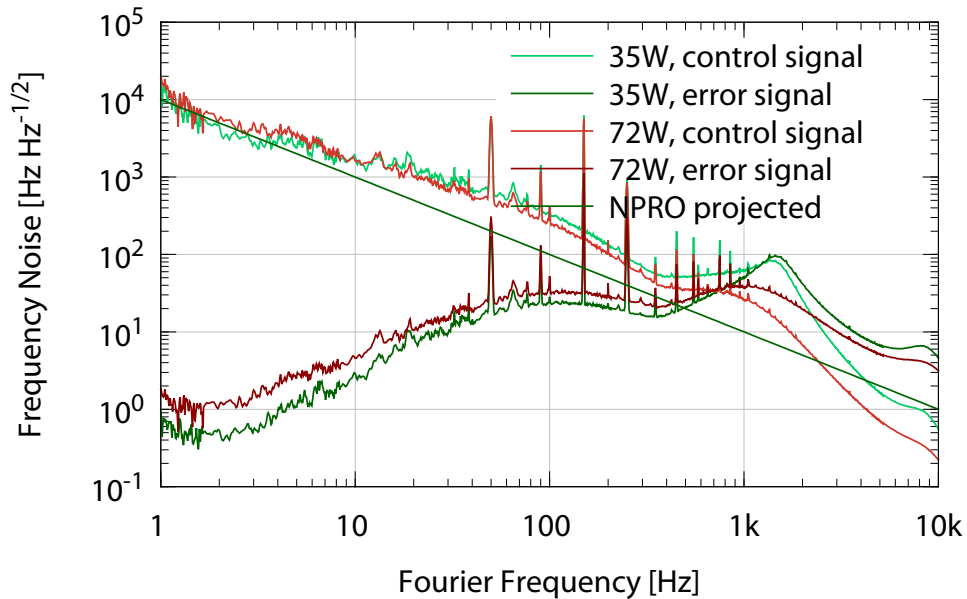
Fig. 4.8 Frequency noise of the 35 W amplifier and the 70 W amplifier as well as the projection of the NPRO. The individual noise measurements are divided into the control signal and the error signal. The signal with the higher noise is giving the correct number. It is recognizable that the 70 W amplifier add no additional noise on the 35 W amplifier.

the noise of the system, here is the noise of the 35 W amplifier higher that of the 70 W amplifier.

Pointing noise

For a LIGO laser, it is also interesting how the pointing noise behaves. For this purpose the pointing was measured using the DBB and compared to the noise of the 35 W amplifier. The measurement is shown in figure 4.9. It can be seen that the pointing noise of both lasers on the same level is. This means there is no additional noise added by the 70 W amplifier.

4.3   neoVAN 8 W solid state amplifier

In many applications, a single-frequency master laser with a good beam profile is necessary. For example as a seed source for GWD a Non-Planar-Ring-Oscillator (NPRO) with a maximum output power of 2 W is used. The NPRO combines the overall good noise performance with a relatively high output power of 2 W. While there are other laser sources
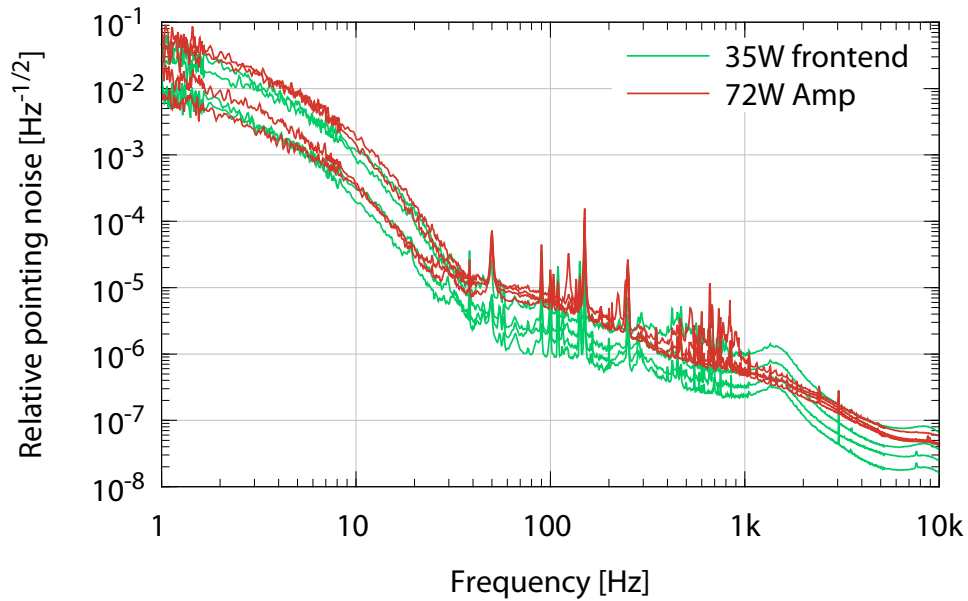
Fig. 4.9 Pointing measurement of the 35 W amplifier and the 70 W amplifier. Both were made with the DBB and the 70 W amplifier add no additional noise on the 35 W amplifier.

with a comparable noise performance, like smaller NPRO or cavity diode lasers, these lasers lack of the necessary output power for many experiments. Within this thesis, a solid state amplifier was used to amplify those low noise lasers and test their performance afterwards. In the next sections two seed lasers, a JDSU NPRO and a RIO ORION diode, were analyzed. With the neoVAN 8 W amplifier the output power was amplified and again analyzed.

4.3.1 RIO ORION laser diode

The RIO ORION laser diode is a laser with an external cavity [Redfern-Integrated-Optics], [30]. The central wavelength is 1064 nm with an output power of 20 mW. The output of the diode is fiber coupled with a FC/APC connector at its end. A picture is shown in 4.10. This diode is interesting as a seed laser for highly stable amplifier systems since the manufacturer promises a very low power noise as well as an ultra-low phase noise. According to its data sheet, the laser should have a narrow line width, smaller than 15 kHz. The wavelength of the system can be modulated via a modulation input. The laser can be controlled and its diagnostics signals can be read out via a computer interface. It is possible to adjust the temperature and thus the wavelength and power of the laser diode.

The laser itself consists of a diode stack which is coated on one side with an high reflective coating, on the other side is an anti reflex coating 4.11. A cavity is formed with the high reflective coating on the diode stack and a the Bragg reflector formed by a planar lightwave circuit, as the output coupler. This light is then collimated by a lens. The length of this cavity is stabilized by a temperature stabilization. [30]

Fig. 4.10 Image of an OEM version of the 20 mW RIO ECDL. It has a wavelength of 1064 nm. The diode is coupled to a FC/APC fiber.
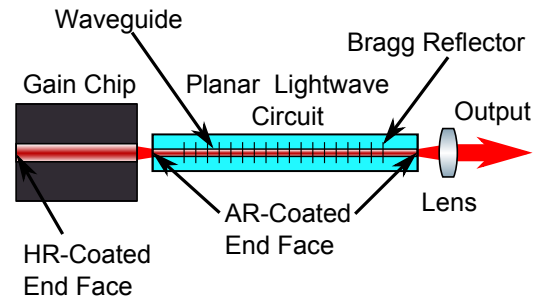
Fig. 4.11 Simple setup of a diode laser with external cavity. The semiconductor chip is anti-reflection coated on one side, and the laser resonator extends to the Bragg reflector formed by a planar lightwave circuit, on the right-hand side.

The output power of the laser can be varied with the temperature of the diode. In figure 4.12 the output power is plotted against the temperature of the diode. It was measured behind a 2 m fiber and the temperature was controlled via the computer interface. At first the power rises linearly with the increase of the temperature up to a maximum of 16 mW. After that a steep drop occurs and the power again rises linearly. Over a temperature range of 15 K three of these slopes were observed. The operating point was set to 293 K with an output power of 16 mW. This temperature was used for the subsequent measurements.

In figure 4.13, a mode scan, measured with the DBB, is plotted of the RIO laser. The proportion of higher order modes is 2.7 %.

4.3.2 JDSU NPRO laser

The second laser is a NPRO laser from JDSU. Is is the model Lumentum NPRO 125N-1064 with a power of 25 mW at a wavelength of 1064 nm. It is a single frequency laser with a linen width of $5\,\mathrm{kHz\,ms^{-1}}$. The laser is shown together with the neoVAN amplifier in picture 4.14.
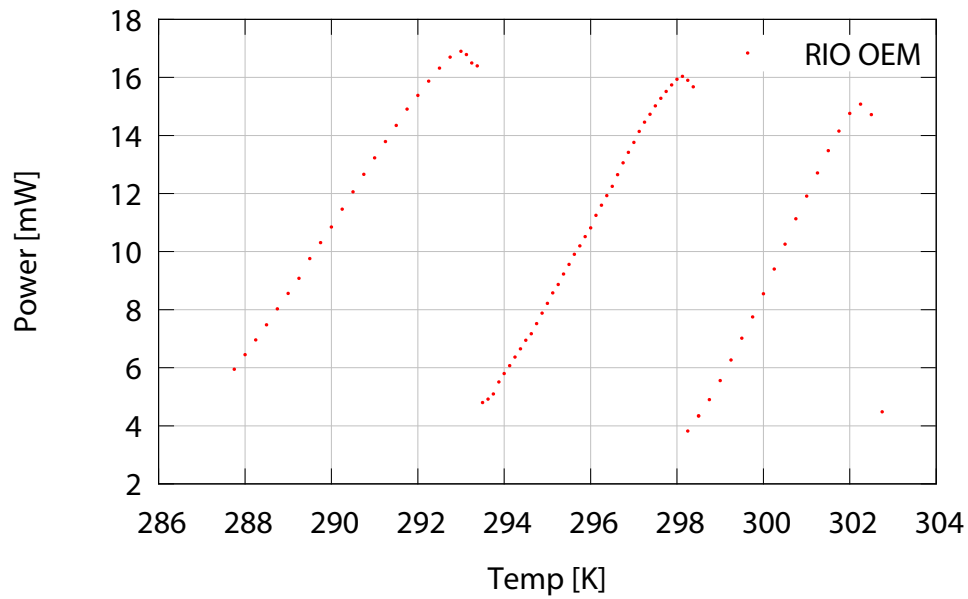
Fig. 4.12 A measurement of the output power of the RIO ORION ECDL, with varying temperature. Three intervals are shown with minimum on the cold side and a maximum on the warm side. The power drop on the warm side is instantaneous.
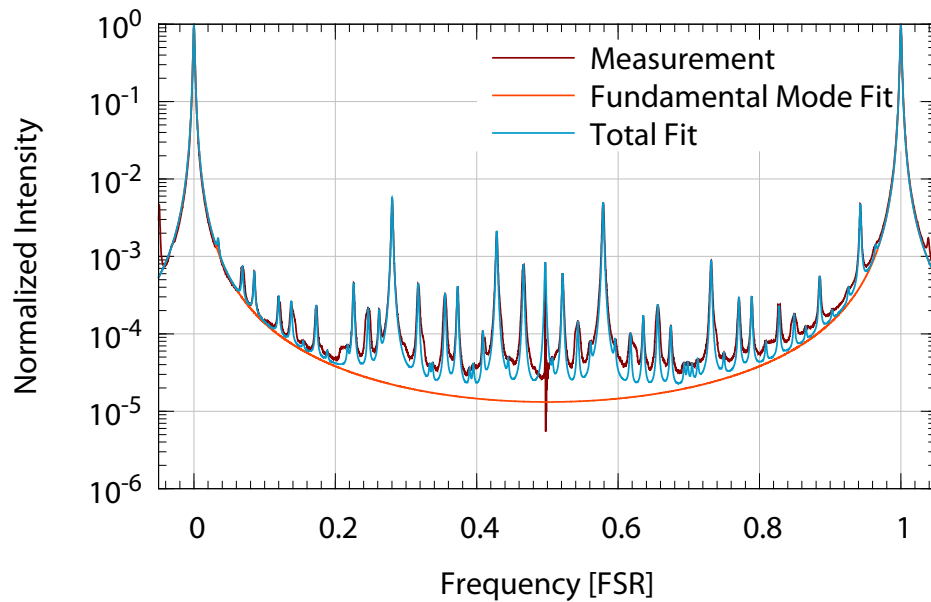
Fig. 4.13 The mode scan of the Rio Diode showing a higher order mode power of 2.7 % and a higher oder mode count of 48.

Fig. 4.14 Picture of the Lumentum NPRO 125N-1064. It is connected by a single mode fiber to a neoVAN amplifier.

The light of the JDSU laser is decoupled from a fiber. With the DBB a measurement of the higher order mode content was taken. It is shown in figure 4.15 and the higher order mode content is 2.4 %.

4.3.3 Fiber coupled solid state amplifier - neoVAN

The amplifier consists of two ND:YVO crystals. The pump diodes with an output power of up to 45 W and a wavelength of 808 nm are connected to these laser crystals via fibers. The input of the amplifier is fiber coupled by a FC/APC connector. The amplifier head and the diode box are water-cooled. The pump current of the diodes and the temperature can be controlled by a web browser interface. The maximum achieved output power was 8 W.

Both seed lasers were now coupled into the amplifier and again the high order mode power was measured. An overview of the set up is shown in picture 4.16. For both measurements, a value of 2.1 % was measured, as plotted in Figure 4.17. The higher oder mode contend is dominated by the single mode fiber and is therefore the same for both laser. The amplifier is conserving it and is not adding additional higher order modes.

4.3.4 Characterization

This section describes the properties of two seed lasers together with the two-stage neo-VAN amplifier, provided by the company Neolase. For this purpose, the two seed lasers were individually measured in power noise and frequency noise. A time series was generated for better comparison. Thereafter, the same measurements were repeated with the amplified lasers. The measurements were then compared to a 2 W NPRO.
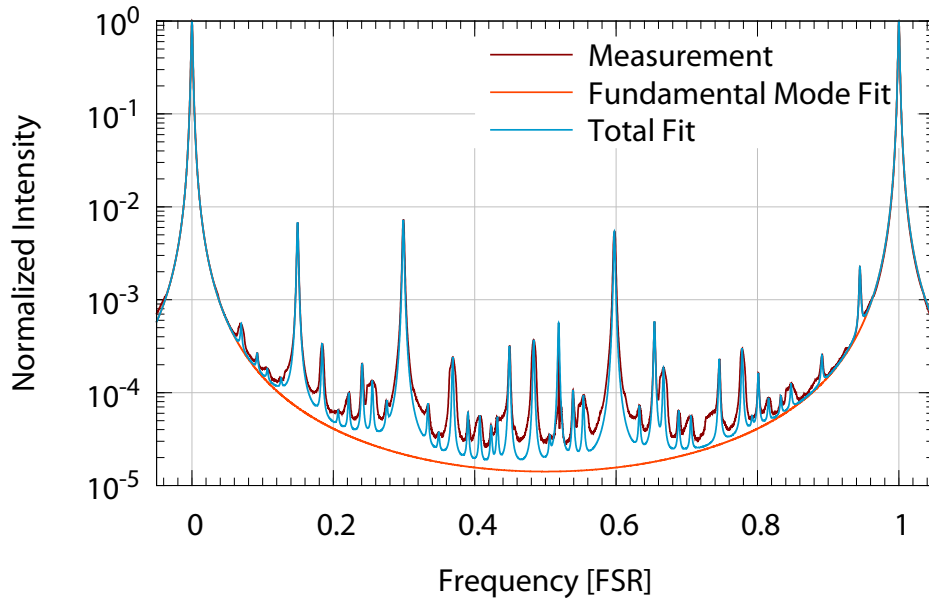
Fig. 4.15 A mode scan of the JDSU NPRO is showing a higher order mode content of 2.4 % and a higher oder mode count of 41.
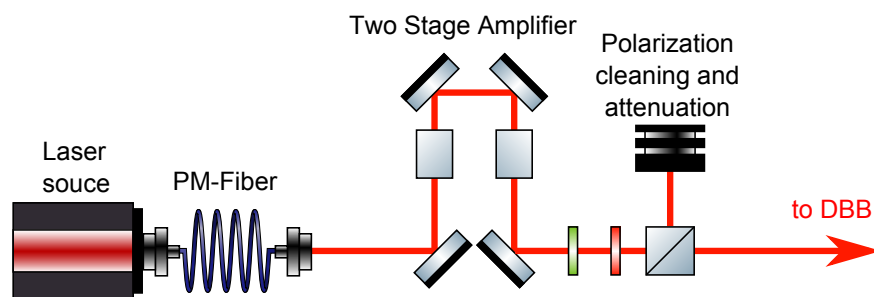
Fig. 4.16 To characterize the neoVAN amplifier the 20 mW NPRO and the 16 mW RIO ECDL were connected via a polarization maintaining single mode fiber. The output light of the amplifier was measured with the diagnostic bread board.
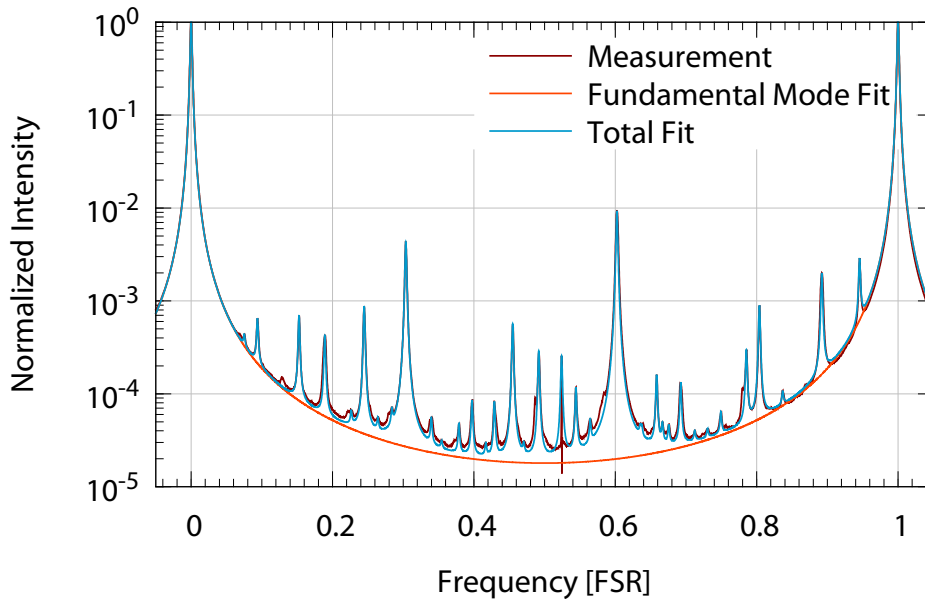
Fig. 4.17 The mode scan of the amplifier showing a higher order mode content of 2.1 %. Both seed lasers where tested and showing the same behavior. It is dominated by the used single mode fiber.

The two different lasers were fed into the diagnostic breadboard. A description can be found in section 4.1. To test the lasers with the DBB the full output power of both lasers was used. For the test of the amplifier, a maximum of 135 mW was injected into the DBB. Before the light is sent to the DBB, the polarization is cleaned and the power attenuated, see picture 4.16.

Relative power noise

The laser power noise is plotted in figure 4.18. In blue, the noise of a 2 W Mephisto NPRO is plotted as a reference. It is $4 \times 10^{-6} / \sqrt{\text{Hz}}$ at 1 Hz and goes down to $2 \times 10^{-7} / \sqrt{\text{Hz}}$ at 10 kHz.

In bright green, the JDSU NPRO is plotted. It has a slightly higher noise at 1 Hz whereby it falls under the noise of the 2 W NPRO from 20 Hz. Up to 3 kHz it is better than the Mephisto NPRO.

The RIO diode, in red, starts at the same level as the JDSU NPRO, but does not drop so strongly. At 100 Hz it has a factor two more noise than the 2 W NPRO. From 1 kHz, all three measurements are in the same order of magnitude. The darker color measurements in red and green are performed with the amplifier. The measurements have a much higher
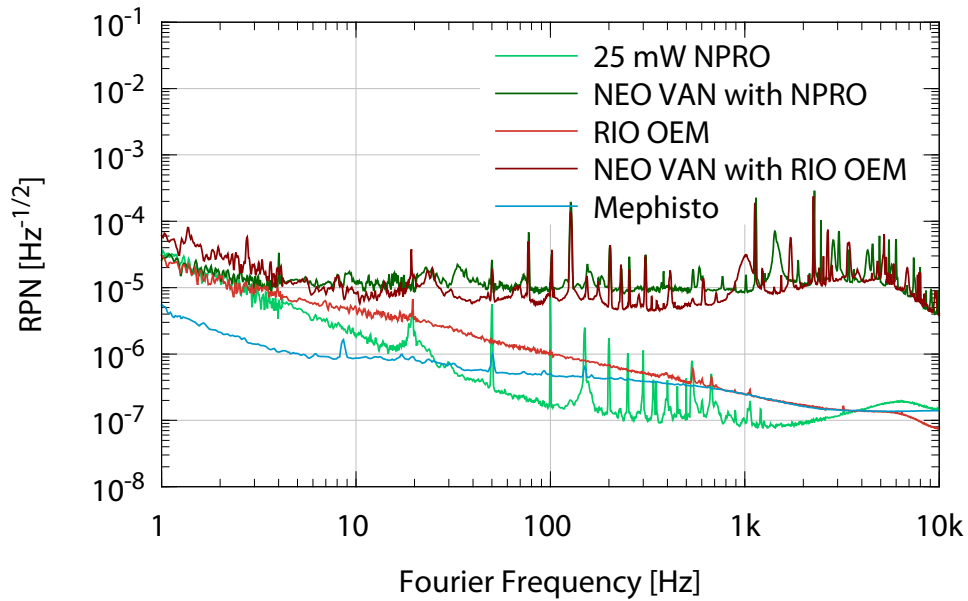
Fig. 4.18 Measurement of the relative power noise of the two seed laser, with and without the neoVAN amplifier. The relative power noise of a 2 W Mephisto NPRO is shown in blue as a reference. The two seed lasers are show in the bright colors of green (JDSU) and red (RIO). Both have a high RPN at low frequencies. The RIO diode is the same as the Mephisto at a frequency of 500 Hz on. The JDSU is even better than the Mephisto, in a frequency range between 30 Hz and 3 kHz. Both amplified lasers have a much higher noise level, probably dominated by the noise of the current driver of the pump diodes.

noise over the entire spectrum, at a level of $1 \times 10^{-5} / \sqrt{\text{Hz}}$. Probably they are limited by the power supply noise of the pump diodes of the amplifier.

Time series

In order to make an estimate about the long-term stability of different lasers, a 300 s time series was taken, see figure 4.19. The color key is the same as before. The scale of the Y-axis is the same in all measurements. The 2 W NPRO has the least variation over the measurement time. Followed by the JDSU NPRO with and without amplifier. The fluctuation of the RIO diode is the biggest. The amplifier reduces the fluctuations slightly.

Frequency noise

One of the most important parameters of the new seed laser is the frequency noise. For this purpose, the frequency noise was measured using the DBB. The measurement is
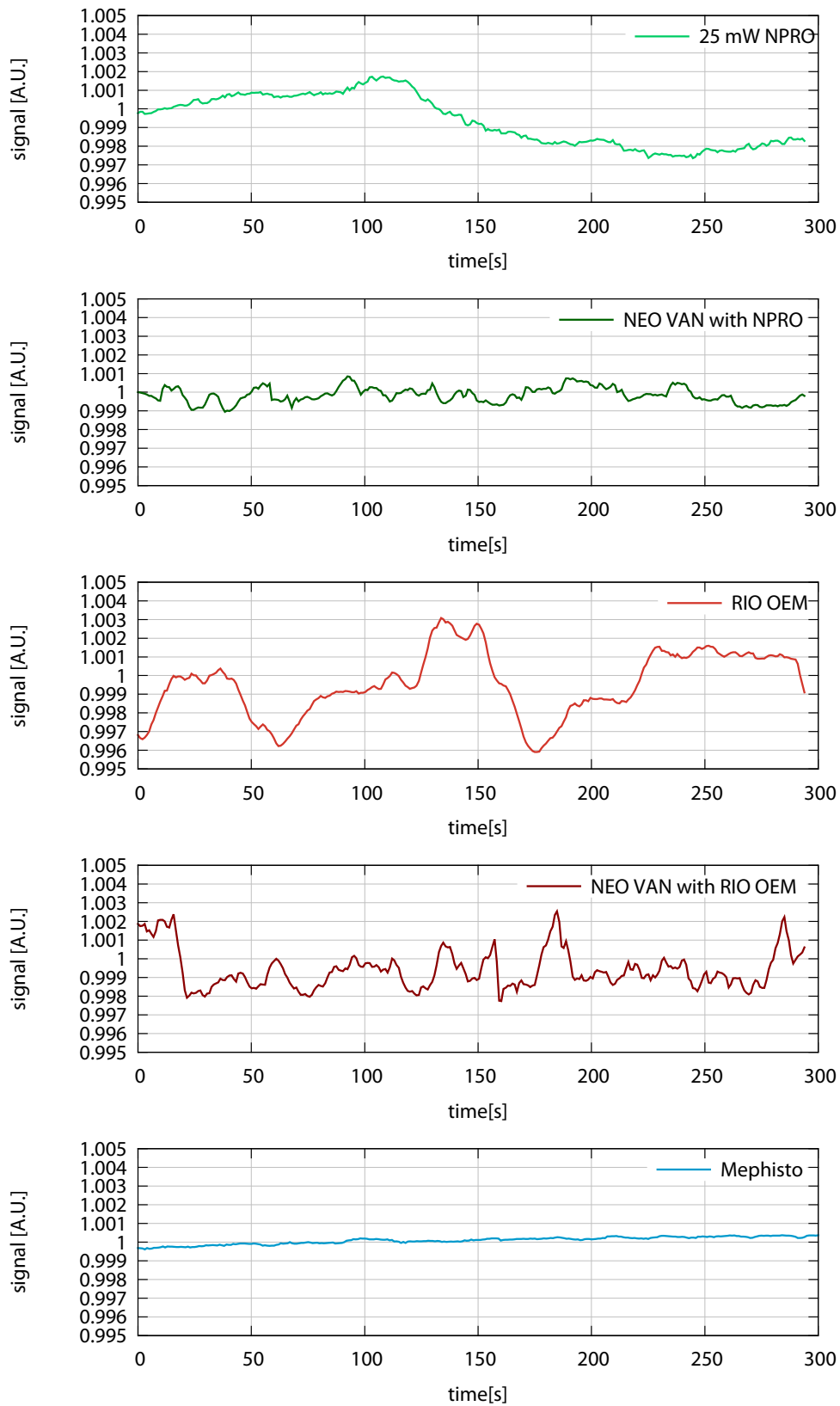
Fig. 4.19 A time series of all five configurations is shown over over a time span of 5 min. The scale of the Y-axis is the same for all measurements. The amplifier is not introducing more deviation in the two new seed lasers. All four are not as stable as the Mephisto.
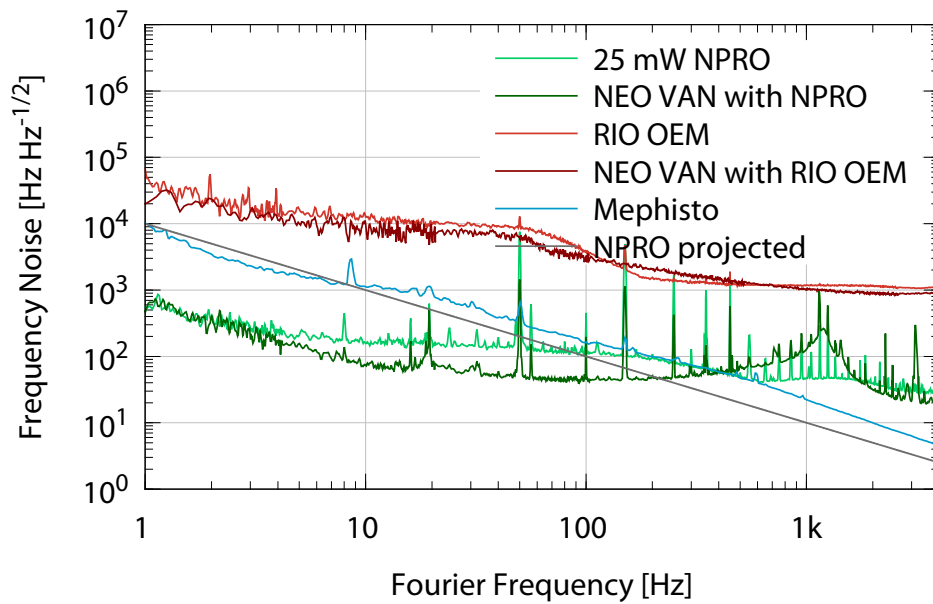
Fig. 4.20 Frequency noise of the two new seed laser and the amplified, compared to a 2 W Mephisto NPRO. The Mephisto in blue has the typical noise of 10 kHz and is falling of with 1/f. The projection is shown in gray. In light green the 25 mW JDSU NPRO is shown. It has a better frequency noise in the lower frequencies. At higher frequencies the noise is above the Mephistos. In dark green, the amplified JDSU NPRO is shown. It has a lower noise in the frequency region between 5 and 400 Hz, without the amplifier. Due to the low input power into the DBB, the gain had to be amplified, and thus a gain amplification of the DBB servo occurred at 1.5 kHz. The RIO diode laser, in red, has a higher frequency noise overall frequencies. It is up to a factor of 50 more than the Mephisto. The amplified laser is almost the same in frequency noise than the diode.

shown in figure 4.20. The color key is the same as for the power noise measurement. As a reference the 2 W Mephisto NPRO and a general projection of NPRO noise, with 10 kHz at 1 Hz and a 1/f drop, is plotted. The results of the measurement with the JDSU NPRO and the amplifier show, that it is even more stable in the range below 200 Hz than the 2 W Mephisto NPRO. At higher frequencies, the noise is above the reference. In red, the two measurements with the RIO diode are plotted. The noise of the RIO diode is much higher, as stated by the company. It is at least one order of magnitude bigger than the Mephisto NPRO. The amplifier does not add additional noise. The frequency noise that is promised in the data sheet from the manufacturer is not reached and thus it is not a replacement for an 2 W Mephisto NPRO.

4.4   Summary

After the recent failure of the HPO at the LIGO Livingston observatory, it still needs to be fully repaired. Within this thesis a possible intermediate solution was found in an solid state four stage amplifier. As a seed for this amplifier, the existing 35 W eLIGO amplifier can be used. With the full 35 W of seed light the output is amplified up to 72 W, while remaining the good beam quality of the seed laser. The analysis of frequency noise, power noise and pointing noise showed that these parameters are conserved by the 70 W amplifier and therefor are better than the high power oscillator [32]. A next iteration of amplifiers designed for 100 W of output power is currently under development. Solid state amplifiers are limited by saturation effects of the amplifier crystals [9].

As a possible replacement for the commercially available 2 W Mephisto NPRO, two small seed laser were amplified with a fiber coupled two stage solid state amplifier from Neolase and analyzed. This configuration can even deliver up to 8 W of output power. The combination of a 20 mW JDSU NPRO and the neoVAN amplifier has excellent frequency noise, and is a good alternative to the Mephisto NPRO, when more power is required. The power noise of the neoVAN amplifier is still higher, and probably could be improved by better current drivers for the pump diodes.

Chapter 5

Fiber Amplifier

Most high precision measurements require a very stable and robust light source. The Einstein Telescope, a third generation gravitational wave detector [36], will be using a continuous wave 500 W laser at a wavelength of 1064 nm for the high-power room temperature high-frequency interferometer. Very strict requirements have been placed on to the frequency and power stability as well as to the spatial beam profile. A possible first approach is an all-fiber single frequency amplifier with an output power of at least 180 W [41]. The first step towards the stabilization of such a fiber based laser system is a complete characterization. The advantage of this laser system compared to traditional solid state systems is the use of new actuators for power stabilization. A combined active and passive stabilization scheme will be essential to meet the requirements.

5.1   Layout of the 180 W Fiber Laser

The experimental setup consists of a non planar ring oscillator (NPRO) as the seed laser, a fiber pre amplifier and an all fiber counter-propagation pumped high power fiber amplifier stage. A picture of the actual fiber laser is shown in 5.2. The NPRO (Innolight Mephisto) emitted up to 2 W of continuous wave single-frequency output power at a wavelength of 1064 nm. The line width of the NPRO is specified with 10 kHz. A detailed sketch is shown in figure 5.1. A detailed description of the pre amplifier can be found in section 5.1.2 and of the main amplifier in section 5.1.3.
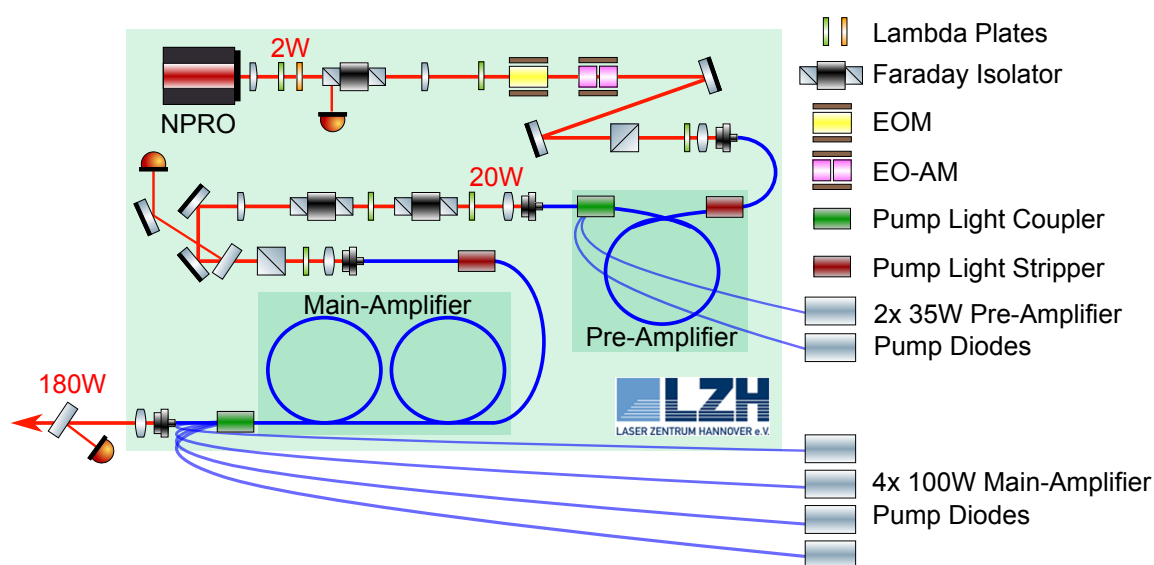
Fig. 5.1 A detailed sketch of the fiber amplifier. Starting with a 2 W NPRO at 1064 nm, the polarization of the light is cleaned by a Faraday isolator. The light passes through, an electro-optic modulator and an electro-optic amplitude modulator before it is transmitted through a polarizing beam splitter. The light is then coupled into the pre amplifier with an efficiency of 65 %. Since both amplifiers are backwards pumped, the pump light stripper is the first component in the active fiber. The active ytterbium doped fiber of the preamplifier is 3 m long and has a core diameter of 10 μm. The pump light coupler brings the 976 nm light into the active fiber. The laser light is coupled out and passes through two Faraday isolators and is fed into the main amplifier. The coupling efficiency is 60 %. The main amplifier can be pumped with four pump diodes, each with 100 W of 976 nm light.

5.1.1   Counter-propagating pumped Laser Amplifier

The concept of a reverse pumped amplifier was used for the two amplifier stages. With this technique the main amplifier is, at the pump powers used in this system, not limited by stimulated Brillouin scattering. The other big advantage is the distribution of pump light in the active fiber. Due to the amplification in the fiber, the amount of 1064 nm seed light increases over the length of the fiber. The pump light comes from the end of the fiber, and as it is converted into the seed light, the amount of pump light decreases towards the front of the fiber. The distribution of seed light to pump light is therefore advantageous. The residual pump light is extracted by a pump light stripper. The pump light is running in the pump core, witch is around the active core. To extract it, the pump core is cut and the light is dumped onto a heat sink [6]. It must be ensured that a seed laser with enough power is always available. Otherwise the pump light is not sufficiently reduced and the risk of damaging the pump light stripper is significant. A further problem is the buildup of a giant pulse which then destroys the end faces of the fiber.

5.1.2   Pre Amplifier

To generate sufficient seed light for the high power amplifier, the NPRO output had to be amplified beforehand. Therefore a pre amplifier was installed. It is made out of a 3 m long ytterbium doped polarization-maintaining fiber (Nufern-PLMA-YDF-10/125-VIII). The 2 W NPRO is used as a seed for this pre amplifier and the light is amplified to 20 W. The seed light is coupled into the 10 μm fiber via high-power coupler, with an efficiency of up to 70 %. The light passes through the pump light stripper into the active fiber. At the other end of the fiber is a 2 + 1/1 pump light coupler, which was developed at the LZH [42]. This couples the light of two pump diodes into the pump core of the fiber. Each with 25 W of output power at a wavelength of 976 nm. The amplified light is then coupled out via a high power connector. In order to protect the preamplifier from backscattering or pulsing of the main amplifier, two Faraday isolators are placed behind its output. The power of the preamplifier is measured by a photo diode behind the Faraday isolators. This photo diode can also be used to stabilize the power of the preamplifier.

5.1.3   Main Amplifier

For the high power amplifier stage, a polarization maintaining Ytterbium doped double-clad (DC) fiber (Nufern-LMA-YDF-25/250-VIII) is used. It is specified with a core diameter
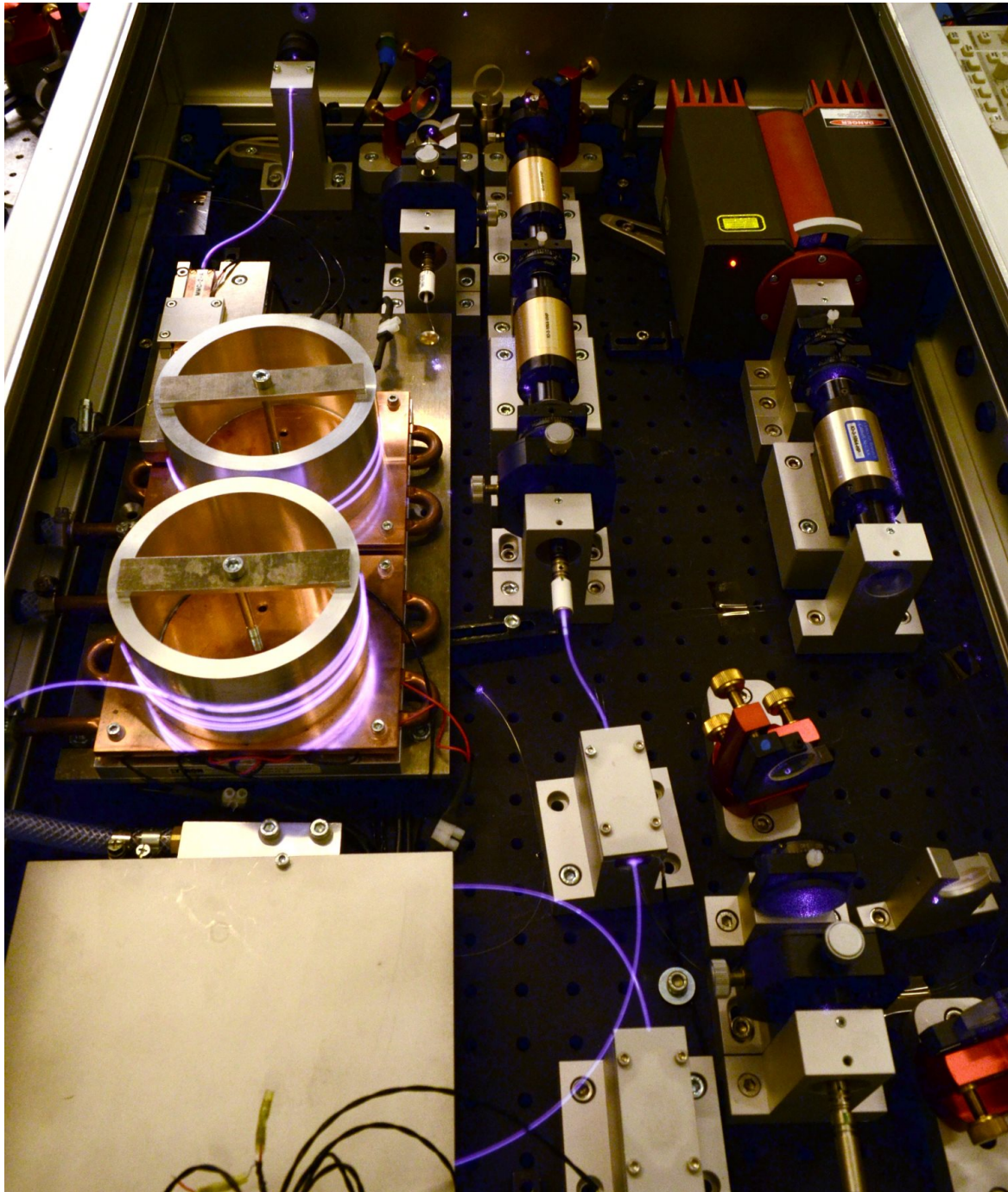
Fig. 5.2 The image shows the fiber amplifier. The NPRO is in the rear right and the pre amplifier in the bottom left. The two coils on the left side hold the main amplifier fiber and are key feature to suppress stimulated Brillouin scattering. The photo was taken with a camera without an IR filter so that the NPRO seed beam can be seen in the fibers.

of 25 μm, a numerical aperture of 0.06 and a cladding diameter of 250 μm, resulting in a numerical aperture of 0.46. The cladding absorption at a wavelength of 976 nm is specified with 4.80 dB m^{-1}. For counter-propagating pump light in the 2.75 m long active fiber, an 4 + 1/1 combiner based on the side-pumping technique, is used [42]. It consists of an active fiber (Nufern-LMA-GDF-25/250) surrounded by four tapered pump fibers. With this setup it is possible to pump the active fiber with four pump diodes. Each diode can emit 100 W at a wavelength of 976 nm. To avoid the occurrence of stimulated Brillouin scattering [8], the active fiber is wound around two coil towers and a temperature gradient is applied. The light from the main amplifier is then collimated via a 15 mm lens. The cladding modes of the active fiber are cut out with an aperture outside of the laser box. A 1 % transmissive mirror is used to attenuate the light for the measurement with the diagnostic breadboard. The rest of the light is transmitted trough a Faraday isolator. A second transmissive mirror is placed behind the Faraday isolator and provides a tap off for the main amplifier photo diode. This monitors the laser power and is also used as a sensor for an initial power stabilization. A detailed sketch can be found in figure 5.3.

5.2   Laser amplification Ratio

The first interesting parameter of a laser amplifier is its amplification ratio. For this purpose, the applied pump current is plotted against the output power of the fiber laser. The two amplifiers were measured individually.

5.2.1   Pre Amplifier

The pre amplifier is directly seeded by the NPRO. 1.5 W of the NPRO power are coupled in with an efficiency of 70 % into the pre amplifier. The two built-in pump diodes are controlled by a Beckhoff system. They are supplied with one current driver and temperature stabilized with one temperature controller. It is only possible to cool the diodes so that the diodes must heat themselves. This results in a system where the pump light can only be slowly raised. Otherwise, the pump light deviates in its wavelength and can not be converted into seed light. It would lead to heat issues at the pump light stripper. Therefore, the measurement was started at the maximum amplification and then decreased. The measurement is shown in figure 5.4. The maximum power of the preamplifier is 22 W with a pump current of 8.8 A. When the current is reduced, the temperature is still optimal,
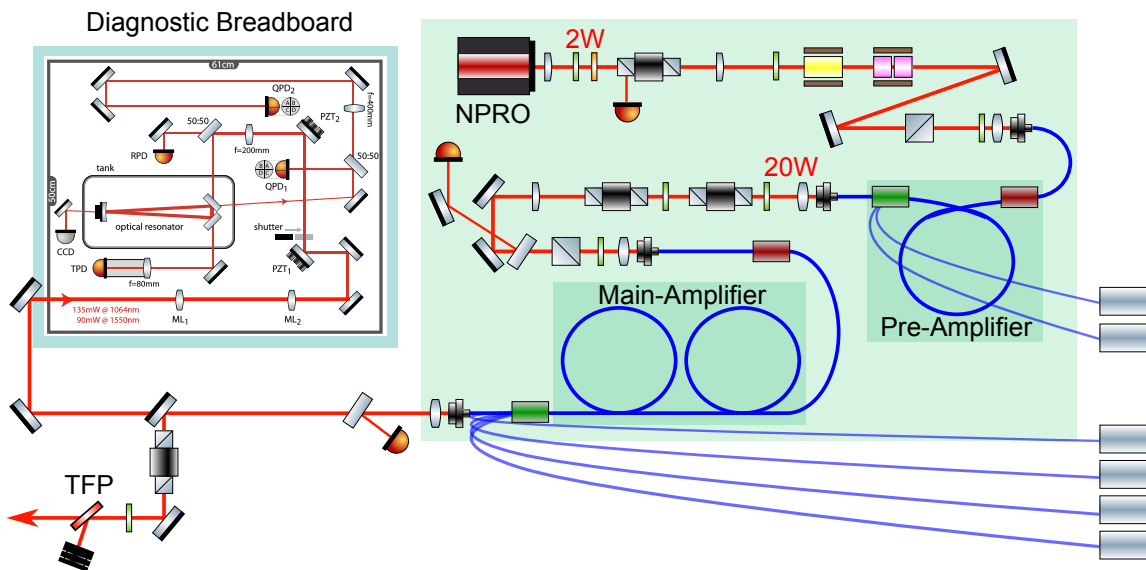
Fig. 5.3 Detailed sketch of the fiber amplifier and the used laser diagnostic. After the laser is coupled out of the Main Amplifier a 15 mm aspherical lens is used to create a 1 mm diameter laser beam. That beam is than sent into a high power Faraday Isolator (ISO-FRDY-08-1064-N). Before this a 1 % pickoff is sent to the CDS controlled DBB for automatic measurements. Behind the FI is another pick-off of 0.1 % that is going to the main amplifier photo diode. This is used for monitoring, but can also be used to power stabilize the laser. The main beam further passes through a lambda half wave plate and a thin film polarizer as an attenuation unit. From there on the beam goes to the aLIGO high power PMC.
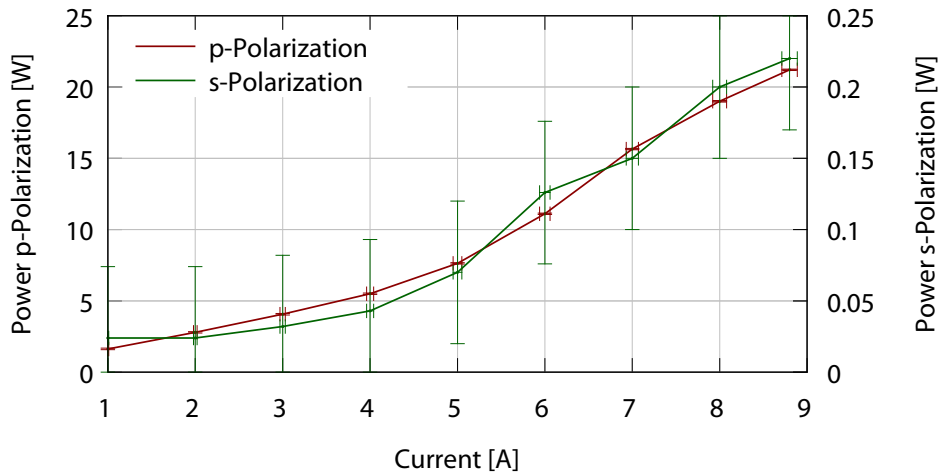
Fig. 5.4 The graph shows the amplification ratio of the pre amplifier. The output power is plotted against the pump current of the pre amplifier. 1.5 W of the NPRO power was sent into the fiber. The coupling efficiency was 70 % and the pump light has a wavelength of 976 nm. At 8.8 A, the amplifier produces 22 W of laser light at 1064 nm.

down to a pump current of 6 A. After that the diodes can not keep the temperature high enough and the curve kinks.

5.2.2 Main Amplifier

The main amplifier is seeded by the pre amplifier. However, the whole 22 W can not be coupled into the main amplifier. There are two Faraday isolators with a combined transmission of 92 %. Only 15 W of light reach the main amplifier. An anti-reflective coated window sends a small portion of the light to the pre amplifier photo diode, which is used for monitoring and power noise analysis. The coupling efficiency into the amplifier is about 65 %. If the main amplifier is not pumped, 10 W of power is transmitted. The measurement of the main amplifier is made in two steps. First, each diode was used individually, as a pump for the amplifier. The measurement is plotted in figure 5.5. Three of the diodes show very similar behavior. Diode 1 is about 10 % more efficient. This is due to the exchange of diode 1 in an earlier phase. With this new pump diode at the maximum current of 10 A the pre-amp could be amplified to 75 W 1064 nm light. The three other diodes amplify to 66 W of output power. For the second measurement, diodes 1 and 4 were used. The maximum power at 10 A pump current for these two diodes was 132 W. The operation point for subsequent measurement is at 120 W or 9 A pump current.
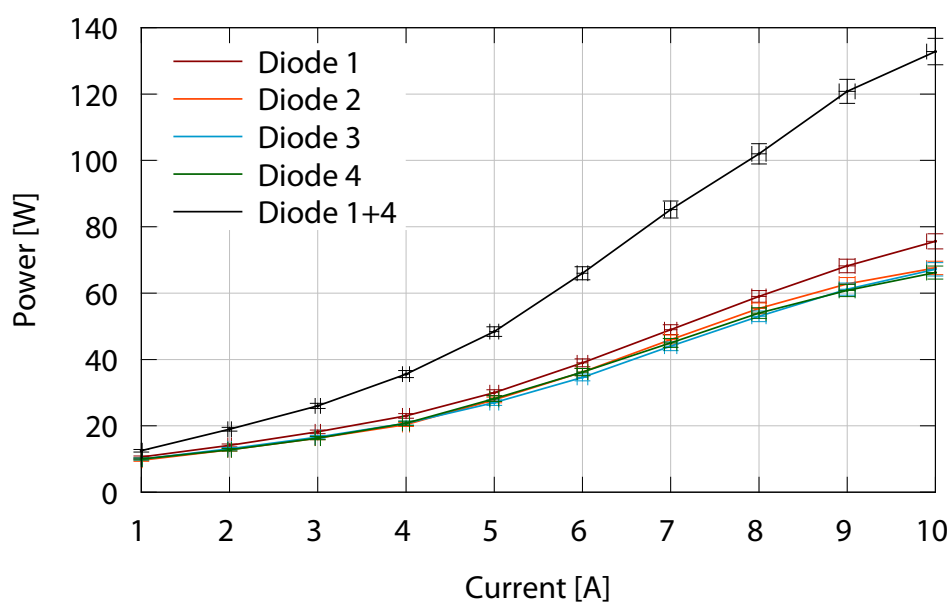
Fig. 5.5 The graph shows the amplification ratio of the main amplifier. 10 W of seed power are coupled through the main amplifier. All four pump diodes are shown individually. Diodes 2, 3 and 4 show the same behavior, while diode 1 is 10 % more efficient. At a pump current of 10 A, 66 W are reached. Diode 1 achieves a higher power with 75 W. In addition, the measurement of diode 1 together with diode 4 is plotted in black. A maximum power of 132 W at 10 A could be achieved.
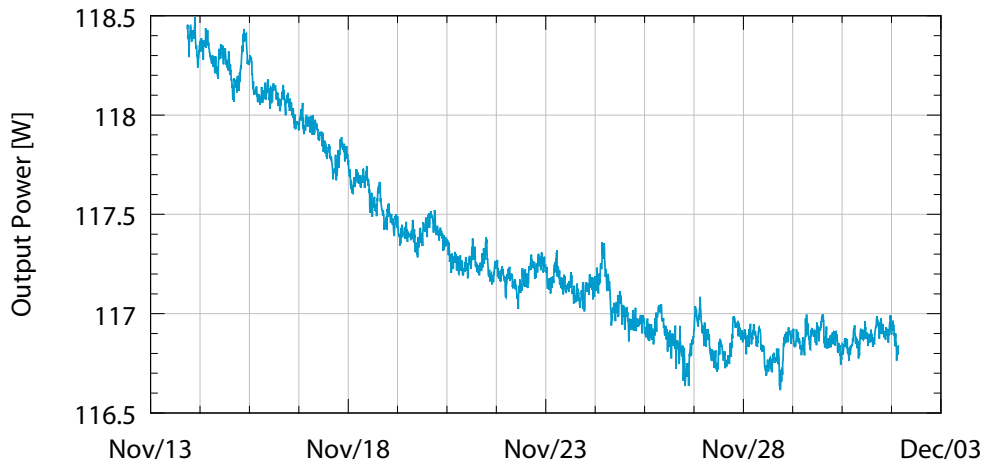
Fig. 5.6 20 day measurement of the main amplifier output power. The main amplifier was pumped with two diodes. The loss of output power was due to a drift of the in coupling to the main amplifier and could be be retrieved by alignment optimization.

5.2.3 Long term behavior

The fiber laser has been operated for 20 days at a power of 120 W. During this time, the power of the laser has dropped by only one percent. By adjusting the in coupling to the main amplifier the original power level was reached again. The measurement is shown in figure 5.6.

5.3 Characterization

To characterize the fiber laser, the power noise as well as the frequency noise and the spatial beam profile are measured. Additionally the beam position fluctuation is a very important parameter and needs to be measured.

5.3.1 Modescan

The active fiber used for the main amplifier has a core diameter of $25\,\mu$m. This is larger than standard single mode fiber for 1064 nm laser. This allows for the higher order modes to pass the fiber. Therefore, the portion of higher modes was measured. The triangular mode filter of the diagnostic breadboard is used for this measurement 4.1. The incoming beam is decomposed into the eigenmodes of the mode filter and thus a statement about
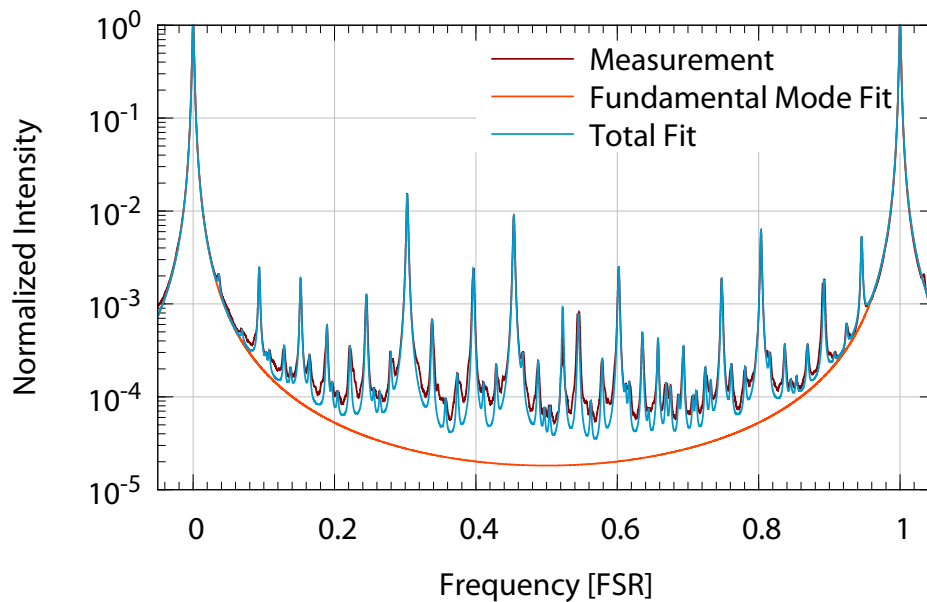
Fig. 5.7 Measurement of the higher order mode content of the fiber laser. The graph shows three different curves, the dark red being the actual measurement. Light red and blue show fit curves. The total higher oder mode content in the fiber laser, operated at 120 W laser power, is 6 % .

the mode purity can be made. The fiber amplifier was operated for these measurements with a power of 120 W and a pick-off beam was sent into the DBB. The measurements showed that the main amplifier has a higher order mode content of 6 % and can be seen in figure 5.7.

5.3.2   Relative power noise

A power noise measurement was performed with the diagnostic breadboard. With the RPD 65 mW of laser light was detected and read out using the CDS. As a comparison for the power noise, a measurement with the free-running high power oscillator of the aLIGO PSL with an output power of 180 W was made. The power of the fiber amplifier was 120 W. For these measurements, the measurement in the frequency range between 1 Hz and 10 kHz was of particularly interest since it is the measurement band of gravitational wave detectors. The measurement, in figure 5.8, showed that at low frequencies from 1 Hz to 100 Hz the fiber amplifier is roughly two orders of magnitude better than the aLIGO laser. The noise at 1 Hz is 3×10^{-5} /$\sqrt{\text{Hz}}$ and decreases with a slope of 1 / f. The fiber laser is affected less since the water cooling is not directly attached to the fiber. A preliminary test with power stabilization was performed and are discussed in detail in section 5.6.
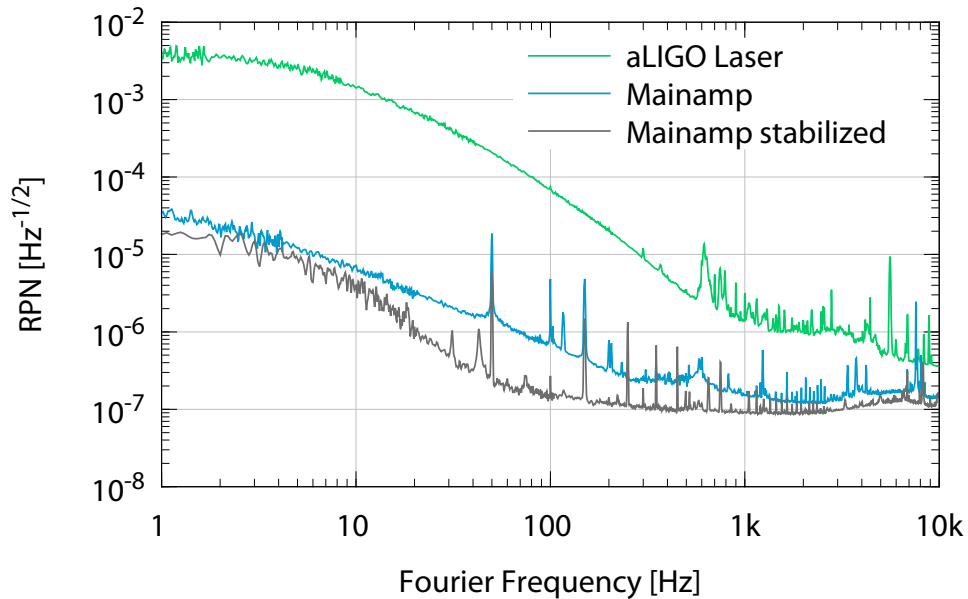
Fig. 5.8 Measurement of the relative power noise, plotted against the Fourier frequencies. The plot shows three graphs, in green the free running aLIGO laser and in blue the fiber amplifier at 120 W. First experiments with the stabilization of the fiber amplifier have been performed and are displayed in gray.

5.3.3 Frequency noise

In Figure 5.9 the projected frequency noise of the 2 W NPRO is plotted as a reference. Three measurements were performed with the fiber laser. First the NPRO without pump light applied to the two amplifier stages. In the second measurement the pre amplifier was pumped the full pump power. The main amplifier was not pumped. Finally, the fully running fiber laser was measured at 120 W of output power. A measurement of the aLIGO high power oscillator is also plotted. At low frequencies of 1 Hz to 10 Hz, all four measurements follow the projection of the NPRO. In the range of 10 Hz to 100 Hz, all configurations are more noisy than the projection. From then on the HPO follows the projection up to 20 kHz. The three fiber amplifier measurements are less noisy in the range of 100 Hz to 10 kHz than the projection. The fully pumped amplifier shows the best noise performance, and is better by a factor of 8 at a frequency of 1 kHz. One possible explanation for this effect could be the doping of the fiber. The active fiber is doped with ytterbium, creating an energy level close to 1064 nm. The cross section between this level and the seed light could be smaller then the linewidth of the NPRO. Another effect could be the thermal coupling of the environment to the fiber. With low pump power the fiber is cooler then with high power, therefore the temperature deviations of the environment
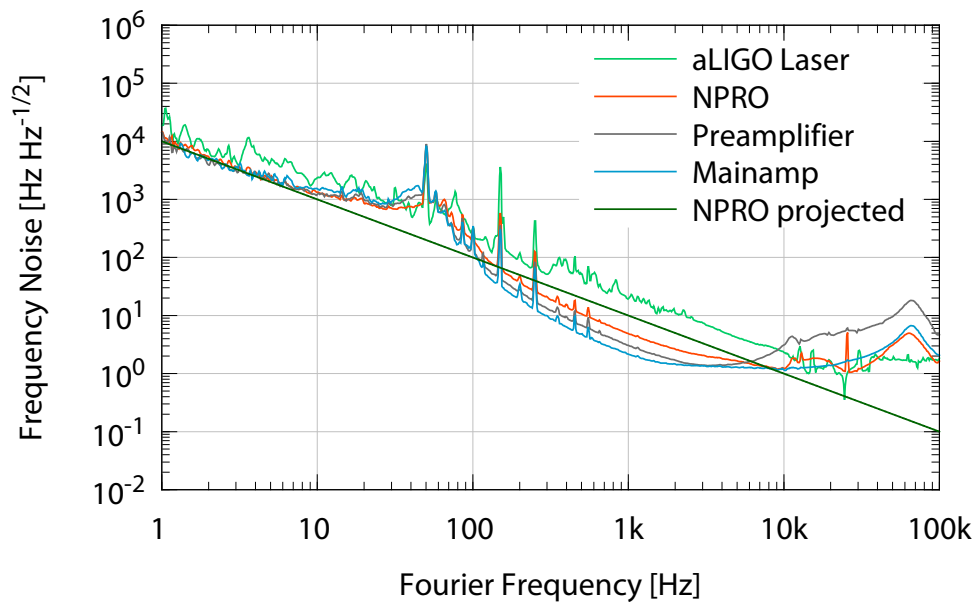
Fig. 5.9 Measurement of the frequency noise of the fiber laser. The typical behavior of an NPRO is shown in dark green, with a noise of 10 kHz at 1 Hz and a 1/f slope. As an additional reference, a measurement of the free running aLIGO high power oscillator is plotted. The fiber laser is characterized by three measurements. In red a measurement of the NPRO, passing through the two non pumped amplifiers. In gray the pre amplifier is pumped and the main amplifier is not. The fully operated fiber laser with 120 W output power is shown in blue. In the frequency range between 1 Hz and 100 Hz, all measurements lie one on top of each other and following the theoretical projection of the NPRO. Between 100 Hz and 10 kHz, the fiber laser is less noisy. Over 10 kHz it is more noisy and has noise amplification due to low phase margin at 80 kHz.

couple more into the fiber length change. This causes more frequency noise. At 60 kHz, noise amplification due to low phase margin can be seen in all measurements of the fiber laser.

5.3.4 Pointing noise

The pointing behavior of a laser is especially interesting for use in an interferometer. The beam fluctuations can be converted into power noise by an optical resonator. The relative pointing noise was measured again with the diagnostic breadboard. In figure 5.10, a comparison between the aLIGO high power laser and the fiber laser can be seen. For comparability, the measurements were made on the same optical table, so that the conditions are the same. At low frequencies, the pointing noise of the fiber laser is much smaller, by two orders of magnitude, than the high power oscillator. From 200 Hz on, both
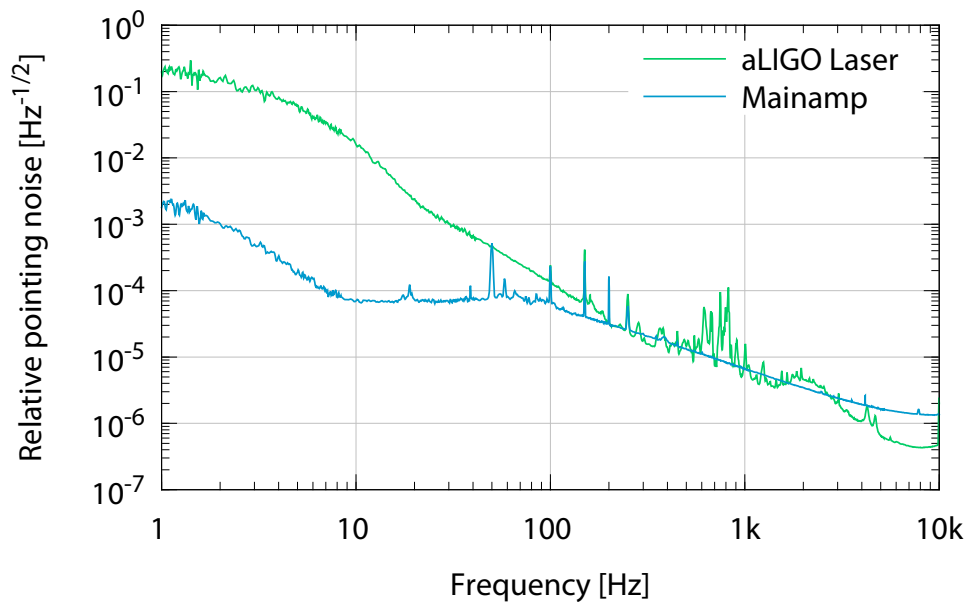
Fig. 5.10 Measurement of the relative pointing noise. The aLIGO high power oscillator is compared to the fiber laser with an output power of 120 W. In the low frequency range between 1 Hz and 100 Hz, the fiber amplifier is much quieter than the high power oscillator. It is up to two orders of magnitude better. In the range of 100 Hz to 3 kHz, they are at the same level. It is assumed that there are many resonances in the relative pointing noise of the aLIGO laser due to the water cooling.

lasers are equally. The resonances caused by the water cooling of the high power oscillator stick out at 500 Hz to 1 kHz.

5.4 Problems and Failures

One of the most important characteristics of a laser system is its reliability. This is why one of the main concerns, is testing the amplifier over long periods of time, with the fiber laser running at high output powers for as long as possible. Before operating the fiber laser at its desired output power of 180 W, a 20 day long test period with an output power of 120 W was performed. To achieve the final output power, three of the four pump diodes were operated at 90 % of their maximum current. During the power increase, the power was stepwise raised from 120 W to 180 W. The first step was 20 W and has always been without any problem. However, when the power was increased to 160 W, the fiber laser broke twice. A third malfunction happed during a power outage. The first problem occurred at the pump light combiner. This was due to screw holes that were contaminated with oil from

the manufacturing process. The oil creped into the fiber when the pump light combiner was heated. The pump light guide in the fiber can no longer function, since the conditions for the total reflection at the glass air interface no longer apply. The second failure, again occurred at the steps from 140 W to 160 W of output power. This time it is not clear what was causing the malfunction. One possibility is that the internal stress of the fiber caused the problem. However, this time the newly implemented automatic shutdown functioned. This easily allowed identification of the place where the fiber was damaged. The third malfunctioning was caused by a power outage. The input coupler of the pre amplifier was broken. This was caused by the fast shut down of the seed laser, resulting in a buildup of a giant pulse which then destroys the end faces of the pre amplifier fiber. During the renewing off the pre amplifier in coupler, the active fiber was then damaged and therefore needed to be shortened. After the successful coupling of seed light back into the fiber, however, due to the length of the fiber, the pump light stripper was overloaded and thus a new failure of the pre amplifier occurred. A further repair could not be carried out during this thesis.

5.5   Improvements

Fiber laser often suffer from stimulated Brillouin scattering. This effect limits the absolute output power. For this fiber laser, two fiber spool towers are built into the main amplifier stage. A temperature gradient between the two towers is created by two temperature controllers. The cold coil is running at 16 °C and the warm one at 36 °C. The two temperature controller can deliver up to 100 W of power, which is applied to the Peltier device underneath the individual towers. With the temperature gradient, the stimulated Brillouin scattering was negligible.

To monitor all relevant parameters and to have long term data acquisition, an aLIGO control and data system (CDS) was set up. This not only eases the data management, but also allows an easy integration into the aLIGO reference system and the use of the diagnostic bread board.

The fiber laser is a prototype, and it is very important, in case problems or malfunctions occur, to improve the design, by structural measures or procedures. With each problem, which occurred during the operation of the fiber laser, attempts were made to make improvements to prevent the problem reoccurring

These included water cooling of the pump light combiner and the pump light stripper of the main amplifier. Even after a short use of the fiber laser it was clear that the thermal management was not optimal. Therefore the two critical components were equipped with better cooling. The pump light combiner was, in the original version, only air-cooled and attached to an aluminum block. This was exchanged to a water-cooled copper block. No temperature problems occurred at this component again. The second critical component is the pump light stripper. In the original design, an aluminum heat sink with water cooling was installed. The heat extraction was insufficient and it was built in a way such that it was not possible to reach it without disassembling the pre amplifier. Therefore, a better heat sink made out of copper was installed. Monitoring of the residual pump light of the main amplifier was additionally set up.

The mounting of the Faraday isolators and lambda plates needed to be improved. For this, all rotation mounts were exchanged to Thorlabs RSP1, resulting in a smoother and more precise adjustment of the lambda plates. Additionally thermal drifts of the rotation mounts and therefore the power drifts could be reduced. For a better adjustment of the beam path inside the fiber laser, the Faraday isolators were placed onto the four-axis tables 9071-M from Newport.

A system for implementation of security watchdogs, including photo diodes for power monitoring and digital control signals, was set up. To circumvent the issue of losing the seed laser for the pre amplifier an uninterpretable power supply for the NPRO laser was installed, and a hierarchy for the power shut down of the amplifier stages was introduced.

5.6 Stabilization

To reach the necessary requirements for gravitational wave detectors, stabilization in the relative power noise, frequency noise and the spatial beam profile have to be applied to the fiber laser. The relative power noise was measured by a photo detector behind the laser box of the fiber laser. This signal was used for an initial test of the power stabilization. For the remaining measurements and stabilizations, the existing stabilization loops of the aLIGO high power laser reference system should have been used, together with the fiber amplifier actuators. Due to the malfunctioning of the fiber laser only the power stabilization could be tested, in an initial state. The following sections explain the available actuators inside the fiber laser, and the possible points for imprinting the correction signals. Finally, the realized power stabilization and its performance is presented.

5.6.1 Modulation and Attenuator

Three options for the power stabilization of the fiber amplifier are installed. The NPRO used as a seed laser has a modulation input for the installed pump diodes. This input has a high actuation coefficient but unfortunately a small bandwidth of only 100 Hz. A second actuator is a current shunt built into the pump diode driver. This is connected to one of the main amplifier pump diode and has the possibility of varying the power of the diode by modulating its current. The last actuator is an electro-optic amplitude modulator from Thorlabs (EO-AM-NR-C2). This is especially designed for high frequencies and can act up to 100 MHz. For the frequency stabilization, the fiber amplifier can be stabilized to the aLIGO reference cavity. First, the light of the fiber laser must be coupled through the aLIGO pre mode cleaner, and is spatially filtered by it. For stabilizing the frequency the same feedback points in the fiber laser are accessible as in the aLIGO high power oscillator. They are using the same model of NPRO laser, and the same electro-optic modulator. The frequency feedback is applied to a 4004 EOM from Newport, for high frequencies. For mid frequencies the feedback is applied to the piezo of the NPRO and for low frequencies it is applied to the temperature of the NPRO crystal.

5.6.2 Sensor

Three sensors are available for power stabilization. First, the monitor photo diode of the pre amplifier. This has also been used for initial stabilization experiments with the pre amplifier [43]. In order to properly stabilize the entire system, the main amplifier monitor photo diode is provided. This is located outside the laser box behind the high power Faraday isolator and was also used for the initial stabilization of the system. This stabilization scheme is further explained in the next section. For later experiments the power stabilization photo diodes of the aLIGO system should be used.

5.6.3 Servo

A servo was designed and built to stabilize the power at the pre amplifier and the main amplifier. The feedback is applied to the current shunt of the laser diode driver of the pre and the main amplifier pump diodes. A detailed description of the servo can be found in [43].

5.6.4   First Results

In figure 5.8, the result of the power stabilization of the fiber laser operated at 120 W is shown. The feedback from the servo was applied to the to the current shunt. The main amplifier photo diode was used as the sensor. This stabilization was not optimized, but it was used as a function test for the actuator. It showed the basic functionality and an improvement of the relative power noise was measured. Unfortunately, there has been a malfunction in the main amplifier and no further experiments could be made within this thesis.

5.7   Summary

As a possible next generation of high power single frequency lasers, a fiber laser prototype from the LZH was under investigation. Its beam parameters were measured and compared with the existing aLIGO high power oscillator. At a power level of 120 W, the fiber laser is equal to the high power oscillator, in terms of frequency noise. The pointing noise of the fiber laser is much better than the one of the aLIGO laser system. Additionally the free running relative power noise, is up to two orders of magnitudes lower and the implementation of power shunts allows an easy application of feedback signals. The introduction of additional acousto-optic modulators is unnecessary. The compact and simple set up of the fiber laser, is making it a desirable option for future gravitational wave detectors. Additionally the fiber laser has a high conversion efficiency of 75 %, in contrast to the aLIGO high power oscillator with an efficiency of only 20 % [33]. A few more improvements have to be applied to the next generation of fiber lasers. The promising measurements of the prototype already make it a auspicious candidate for the next generation of gravitational wave detectors.

Chapter 6

Conclusion

For future interferometric gravitational wave detectors, lasers with an output power of up to 500 W are required. Instead of solid state laser systems, fiber amplification are a promising candidate. Besides total optical power also the power noise, frequency noise, beam pointing fluctuations, and spatial beam parameters have to meet strict requirements.

The current laser system of aLIGO provides frequency and power stabilized light at the specifications required for the input optics chain. The laser system consists of a 2 W non-planar ring-oscillator at a wavelength of 1064 nm, amplified to an output power of 35 W by four Nd:YVO4 crystals pumped at 808 nm. The high power oscillator, contains an injection-locked ring oscillator with four Nd:YAG crystals delivering up to 200 W of output power.

In the Chapter 3, the design and installation of the 35 W eLIGO amplifier, the photonic crystal fiber, the mode filter, and the power stabilization for the the AEI 10 m prototype is described. The experiments at the AEI 10 m prototype require up to 8 W of laser power. By using a photonic crystal fiber a throughput of 20 W is possible without stimulated Brillouin scattering. Additionally, the fiber serves as a mode filter, with 99.8 % in the fundamental mode of the laser beam. To further clean the spacial mode, a triangular spacer mode filter with a finesse of 1000 is installed. For power stabilization, the aLIGO photo diode array was installed and the stabilization to a relative power noise of $2 \times 10^{-9} / \sqrt{\mathrm{Hz}}$ was demonstrated.

In Chapter 4 two types of solid state amplifiers were characterized. The first one is a two stage single frequency Nd:YVO4 amplifier with up to 8 W of output power. As seed lasers, two different fiber coupled laser were used. An external cavity diode laser

and a NPRO laser both with an output power of 20 mW and a wavelength of 1064 nm, were tested and characterized together with the amplifier. It was shown that the power noise is dominated by the pump current of the amplifier, and the good frequency noise is transfered from the seed source to the amplifier. The second amplifier is a four stage solid state system with an output power of 70 W. As a seed source, the aLIGO 35 W amplifier was used. The frequency noise is on the same level as it is for the 35 W amplifier and the power noise is only slightly increased. To have an intermediate solution for the power increase of the upcoming sciences runs, it is planned to implement the 70 W amplifier in the LIGO Livingston observatory. The VIRGO observatory is currently examining the possible use of amplifying a 20 W seed laser with a solid state amplifier to 100 W of output power.

However, the possibilities of solid state amplifiers are almost exhausted and systems, such as the aLIGO high power oscillator are also not suitable for the next generation. Systems with higher power and lower maintenance efforts and higher reproducibility are required.

A fiber based single frequency amplifier was introduced in the chapter 5. In collaboration with the Laser Zentrum Hannover, a two-stage fiber amplifier was developed which consists of a 2 W NPRO as a seed laser and two fiber amplifiers, using ytterbium-doped large-mode-area fibers with a pump wavelength of 976 nm. Both amplifiers have a gain factor of 10 with a high optical-to-optical efficiency of 75 %. The resulting output power is comparable to the aLIGO high power oscillator, delivering up to 180 W. One of the advantages of this laser system is the use of actuators directly controlling the laser output power. For power stabilization, each amplifier stage is equipped with a power-shunt and an EO-AM is modulating the seed laser power. The technical feasibility of a long term stable single-frequency amplifier was shown without photo-darkening or stimulated Brillouin scattering. The fiber laser has a similar performance in frequency noise and spatial beam profile as the aLIGO high power laser. The power noise and beam pointing fluctuation are much better than with the aLIGO laser.

The fiber laser is a possible replacement for the current aLIGO laser. The reliability, however, needs to be improved. The improvement of the fiber laser has already been started within this thesis and a further cooperation between the AEI and the LZH, for developing the next generation of fiber lasers, is established.

One possible solution to achieve the required 500 W of laser power for the third generation of gravitational wave detectors, is to coherently combine two high power lasers. First experiments, combining the aLIGO high power laser and the fiber laser are started.

The further step is to use two fiber amplifiers with an output of 250 W each, and combine both.

References

[1] Abbott, B., Abbott, R., Abbott, T., Abernathy, M., Acernese, F., Ackley, K., Adams, C., Adams, T., Addesso, P., Adhikari, R., Adya, V., Affeldt, C., Agathos, M., Agatsuma, K., Aggarwal, N., Aguiar, O., Aiello, L., Ain, A., Ajith, P., Allen, B., Allocca, A., Altin, P., Anderson, S., Anderson, W., Arai, K., Arain, M., Araya, M., Arceneaux, C., Areeda, J., Arnaud, N., Arun, K., Ascenzi, S., Ashton, G., Ast, M., Aston, S., Astone, P., Aufmuth, P., Aulbert, C., Babak, S., Bacon, P., Bader, M., Baker, P., Baldaccini, F., Ballardin, G., Ballmer, S., Barayoga, J., Barclay, S., Barish, B., Barker, D., Barone, F., Barr, B., Barsotti, L., Barsuglia, M., Barta, D., Bartlett, J., Barton, M., Bartos, I., Bassiri, R., Basti, A., Batch, J., Baune, C., Bavigadda, V., Bazzan, M., Behnke, B., Bejger, M., Belczynski, C., Bell, A., Bell, C., Berger, B., Bergman, J., Bergmann, G., Berry, C., Bersanetti, D., Bertolini, A., Betzwieser, J., Bhagwat, S., Bhandare, R., Bilenko, I., Billingsley, G., Birch, J., Birney, R., Birnholtz, O., Biscans, S., Bisht, A., Bitossi, M., Biwer, C., Bizouard, M., Blackburn, J., Blair, C., Blair, D., Blair, R., Bloemen, S., Bock, O., Bodiya, T., Boer, M., Bogaert, G., Bogan, C., Bohe, A., Bojtos, P., Bond, C., Bondu, F., Bonnand, R., Boom, B., Bork, R., Boschi, V., Bose, S., Bouffanais, Y., Bozzi, A., Bradaschia, C., Brady, P., Braginsky, V., Branchesi, M., Brau, J., Briant, T., Brillet, A., Brinkmann, M., Brisson, V., Brockill, P., Brooks, A., Brown, D., Brown, D., Brown, N., Buchanan, C., Buikema, A., Bulik, T., Bulten, H., Buonanno, A., Buskulic, D., Buy, C., Byer, R., Cabero, M., Cadonati, L., Cagnoli, G., Cahillane, C., Bustillo, J. C., Callister, T., Calloni, E., Camp, J., Cannon, K., Cao, J., Capano, C., Capocasa, E., Carbognani, F., Caride, S., Diaz, J. C., Casentini, C., Caudill, S., Cavaglià, M., Cavalier, F., Cavalieri, R., Cella, G., Cepeda, C., Baiardi, L. C., Cerretani, G., Cesarini, E., Chakraborty, R., Chalermsongsak, T., Chamberlin, S., Chan, M., Chao, S., Charlton, P., Chassande-Mottin, E., Chen, H., Chen, Y., Cheng, C., Chincarini, A., Chiummo, A., Cho, H., Cho, M., Chow, J., Christensen, N., Chu, Q., Chua, S., Chung, S., Ciani, G., Clara, F., Clark, J., Cleva, F., Coccia, E., Cohadon, P.-F., Colla, A., Collette, C., Cominsky, L., Constancio, M., Conte, A., Conti, L., Cook, D., Corbitt, T., Cornish, N., Corsi, A., Cortese, S., Costa, C., Coughlin, M., Coughlin, S., Coulon, J.-P., Countryman, S., Couvares, P., Cowan, E., Coward, D., Cowart, M., Coyne, D., Coyne, R., Craig, K., Creighton, J., Creighton, T., Cripe, J., Crowder, S., Cruise, A., Cumming, A., Cunningham, L., Cuoco, E., Canton, T. D., Danilishin, S., D'Antonio, S., Danzmann, K., Darman, N., Costa, C. D. S., Dattilo, V., Dave, I., Daveloza, H., Davier, M., Davies, G., Daw, E., Day, R., De, S., DeBra, D., Debreczeni, G., Degallaix, J., Laurentis, M. D., Deléglise, S., Pozzo, W. D., Denker, T., Dent, T., Dereli, H., Dergachev, V., DeRosa, R., Rosa, R. D., DeSalvo, R., Dhurandhar, S., Díaz, M., Fiore, L. D., Giovanni, M. D., Lieto, A. D., Pace, S. D., Palma, I. D., Virgilio, A. D., Dojcinoski, G., Dolique, V., Donovan, F., Dooley, K., Doravari, S., Douglas, R., Downes, T., Drago, M., Drever, R., Driggers, J., Du, Z., Ducrot, M., Dwyer, S., Edo, T., Edwards, M., Effler, A., Eggenstein, H.-B., Ehrens, P., Eichholz, J., Eikenberry, S.,

Engels, W., Essick, R., Etzel, T., Evans, M., Evans, T., Everett, R., Factourovich, M., Fafone, V., Fair, H., Fairhurst, S., Fan, X., Fang, Q., Farinon, S., Farr, B., Farr, W., Favata, M., Fays, M., Fehrmann, H., Fejer, M., Feldbaum, D., Ferrante, I., Ferreira, E., Ferrini, F., Fidecaro, F., Finn, L., Fiori, I., Fiorucci, D., Fisher, R., Flaminio, R., Fletcher, M., Fong, H., Fournier, J.-D., Franco, S., Frasca, S., Frasconi, F., Frede, M., Frei, Z., Freise, A., Frey, R., Frey, V., Fricke, T., Fritschel, P., Frolov, V., Fulda, P., Fyffe, M., Gabbard, H., Gair, J., Gammaitoni, L., Gaonkar, S., Garufi, F., Gatto, A., Gaur, G., Gehrels, N., Gemme, G., Gendre, B., Genin, E., Gennai, A., George, J., Gergely, L., Germain, V., Ghosh, A., Ghosh, A., Ghosh, S., Giaime, J., Giardina, K., Giazotto, A., Gill, K., Glaefke, A., Gleason, J., Goetz, E., Goetz, R., Gondan, L., González, G., Castro, J. G., Gopakumar, A., Gordon, N., Gorodetsky, M., Gossan, S., Gosselin, M., Gouaty, R., Graef, C., Graff, P., Granata, M., Grant, A., Gras, S., Gray, C., Greco, G., Green, A., Greenhalgh, R., Groot, P., Grote, H., Grunewald, S., Guidi, G., Guo, X., Gupta, A., Gupta, M., Gushwa, K., Gustafson, E., Gustafson, R., Hacker, J., Hall, B., Hall, E., Hammond, G., Haney, M., Hanke, M., Hanks, J., Hanna, C., Hannam, M., Hanson, J., Hardwick, T., Harms, J., Harry, G., Harry, I., Hart, M., Hartman, M., Haster, C.-J., Haughian, K., Healy, J., Heefner, J., Heidmann, A., Heintze, M., Heinzel, G., Heitmann, H., Hello, P., Hemming, G., Hendry, M., Heng, I., Hennig, J., Heptonstall, A., Heurs, M., Hild, S., Hoak, D (2016). Observation of gravitational waves from a binary black hole merger. *Physical Review Letters*, 116(6).

[2] Affeldt, C. (2014). *Laser power increase for GEO 600*. PhD thesis, University of Hannover.

[3] Alig, T. (2013). *Charakterisierung und Unterdrückung der Strahlgeometriefluktuationen des fasergekoppelten 35W Lasers für das AEI 10m Prototypinterferometer*. Diploma thesis, University of Hannover.

[4] AS, N. P. (2015). Lma 15 single mode 15 μm core fiber. Technical report.

[5] Black, E. D. (2001). An introduction to pound–drever–hall laser frequency stabilization. *American Journal of Physics*, 69(1):79–87.

[6] Boehme, S., Hirte, K., Fabian, S., Hupel, C., Schreiber, T., Eberhardt, R., and Tünnermann, A. (2014). CO2-laser-based coating process for high power fiber application. In Klotzbach, U., Washio, K., and Arnold, C. B., editors, *Laser-based Micro- and Nanoprocessing VIII*.

[7] Bork, R. (2010). Advligo cds design overview ligo-t0900612-v2. Technical report, LIGO Scientific Collaboration.

[8] Chiao, R. Y., Townes, C. H., and Stoicheff, B. P. (1964). Stimulated brillouin scattering and coherent generation of intense hypersonic waves. *Physical Review Letters*, 12(21):592–595.

[9] Fan, T. (1993). Heat generation in nd:YAG and yb:YAG. *IEEE Journal of Quantum Electronics*, 29(6):1457–1459.

[10] Frede, M., Schulz, B., Wilhelm, R., Kwee, P., Seifert, F., Willke, B., and Kracht, D. (2007). Fundamental mode, single-frequency laser amplifier for gravitational wave detectors. *Optics Express*, 15(2):459.

[11] Freitag, I., Tünnermann, A., and Welling, H. (1995). Power scaling of diode-pumped monolithic nd:YAG lasers to output powers of several watts. *Optics Communications*, 115(5-6):511–515.

[12] Fritschel, P. (2008). Advanced ligo systems design. *Technical Report LIGO-T010075-v2*.

[13] Goßler, S., Bertolini, A., Born, M., Chen, Y., Dahl, K., Gering, D., Gräf, C., Heinzel, G., Hild, S., Kawazoe, F., Kranz, O., G Kühn, Lück, H., Mossavi, K., Schnabel, R., Somiya, K., Strain, K. A., Taylor, J. R., Wanner, A., Westphal, T., Willke, B., and K Danzmann (2010). The AEI 10 m prototype interferometer. *Classical and Quantum Gravity*, 27(8):084023.

[14] Harry, G. M. (2010). Advanced LIGO: the next generation of gravitational wave detectors. *Classical and Quantum Gravity*, 27(8):084006.

[15] Junker, J. (2016). *Laser power stabilization for the AEI 10m Prototype*. Master thesis, University of Hannover.

[16] Junker, J., Oppermann, P., and Willke, B. (2017). Shot-noise-limited laser power stabilization for the AEI 10 m prototype interferometer. *Optics Letters*, 42(4):755.

[17] Kane, T. J. and Byer, R. L. (1985). Monolithic, unidirectional single-mode nd:YAG ring laser. *Optics Letters*, 10(2):65.

[18] King, P. (2011). Outer loop power stabilisation final design ligo-t1100265-v1. Technical report, LIGO Scientific Colaboration.

[19] King, P., Willke, B., Savage, R., and Wessels, P. (2008). Psl preliminary design ligo-t080195-v1. Technical report, LIGO Scientific Colaboration.

[20] Kwee, P. (2005). *Charakterisierung von Lasersystemen für Gravitationswellendetektoren*. Diploma thesis, University of Hannover.

[21] Kwee, P., Bogan, C., Danzmann, K., Frede, M., Kim, H., King, P., Pöld, J., Puncken, O., Savage, R. L., Seifert, F., Wessels, P., Winkelmann, L., and Willke, B. (2012). Stabilized high-power laser system for the gravitational wave detector advanced LIGO. *Optics Express*, 20(10):10617.

[22] Kwee, P., Seifert, F., Willke, B., and Danzmann, K. (2007). Laser beam quality and pointing measurement with an optical resonator. *Review of Scientific Instruments*, 78(7):073103.

[23] Kwee, P. and Willke, B. (2008). Automatic laser beam characterization of monolithic nd:YAG nonplanar ring lasers. *Applied Optics*, 47(32):6022.

[24] Kwee, P., Willke, B., and Danzmann, K. (2009a). Shot-noise-limited laser power stabilization with a high-power photodiode array. *Optics Letters*, 34(19):2912.

[25] Kwee, P., Willke, B., and Danzmann, K. (2009b). Shot-noise-limited laser power stabilization with a high-power photodiode array. *Optics Letters*, 34(19):2912.

[26] McClelland, D., Mavalvala, N., Chen, Y., and Schnabel, R. (2011). Advanced interferometry, quantum optics and optomechanics in gravitational wave detectors. *Laser & Photonics Reviews*, pages n/a–n/a.

[27] Morrison, E., Meers, B. J., Robertson, D. I., and Ward, H. (1994). Automatic alignment of optical interferometers. *Applied Optics*, 33(22):5041.

[28] Mueller, G. (2005). Beam jitter coupling in advanced LIGO. *Optics Express*, 13(18):7118.

[29] NeoLase and Frede, M. (2017). Laser amplifier neovanfactsheet. Technical report, NeoLASE.

[30] Numata, K., Alalusi, M., Stolpner, L., Margaritis, G., Camp, J., and Krainak, M. (2014). Characteristics of the single-longitudinal-mode planar-waveguide external cavity diode laser at 1064 nm. *Optics Letters*, 39(7):2101.

[31] Põld, J. H. (2009). Stabilization of the advanced ligo 200w laser. Master's thesis, Gottfried Wilhelm Leibniz Universität Hannover.

[32] Põld, J. H. (2014). *Design, Implementation and Characterization of the Advanced LIGO 200 W System,*. PhD thesis, Leibniz Universität Hannover.

[33] Puncken, O. (2011). *Pumpkopfdesign für den Advanced LIGO Laser*. PhD thesis, Gottfried Wilhelm Leibniz Universität Hannover.

[Redfern-Integrated-Optics] Redfern-Integrated-Optics. 1064 nm rio orion laser module datasheet.

[35] Saleh, B. E. A. and Teich, M. C. (2007). *Fundamentals of Photonics*. Wiley John + Sons.

[36] science team, E. (2011). Et design study document. Technical report, European Gravitational Observatory.

[37] Seifert, F., Kwee, P., Heurs, M., Willke, B., and Danzmann, K. (2006). Laser power stabilization for second-generation gravitational wave detectors. *Optics Letters*, 31(13):2000.

[38] Smith, J. R. (2009). The path to the enhanced and advanced LIGO gravitational-wave detectors. *Classical and Quantum Gravity*, 26(11):114013.

[39] Somiya, K., Kokeyama, K., and Nawrodt, R. (2010). Remarks on thermoelastic effects at low temperatures and quantum limits in displacement measurements. *Physical Review D*, 82(12).

[40] Somiya, K. and Yamamoto, K. (2009). Coating thermal noise of a finite-size cylindrical mirror. *Physical Review D*, 79(10).

[41] Theeg, T. (2015). *Monolithischer Yb-Faserverstärker zur Leistungsskalierung von einfrequenten Laserquellen: Erforschung und Integration eines vollständig faserbasierten Pumplichtkopplers*. PhD thesis, Gottfried Wilhelm Leibniz Universität Hannover.

[42] Theeg, T., Sayinc, H., Neumann, J., Overmeyer, L., and Kracht, D. (2012). Pump and signal combiner for bi-directional pumping of all-fiber lasers and amplifiers. *Optics Express*, 20(27):28125.

[43] Thies, F. (2014). Leistungsstabilisierung eines faserlasers. Master's thesis, Albert-Einstein-Institut Hannover, Leibniz Universität Hannover.

[44] Willke, B., Danzmann, K., Frede, M., King, P., Kracht, D., Kwee, P., Puncken, O., Savage, R. L., Schulz, B., Seifert, F., Veltkamp, C., Wagner, S., Weßels, P., and Winkelmann, L. (2008). Stabilized lasers for advanced gravitational wave detectors. *Classical and Quantum Gravity*, 25(11):114040.

[45] Winkelmann, L., Puncken, O., Kluzik, R., Veltkamp, C., Kwee, P., Poeld, J., Bogan, C., Willke, B., Frede, M., Neumann, J., Wessels, P., and Kracht, D. (2011). Injection-locked single-frequency laser with an output power of 220 w. *Applied Physics B*, 102(3):529–538.

Appendix A
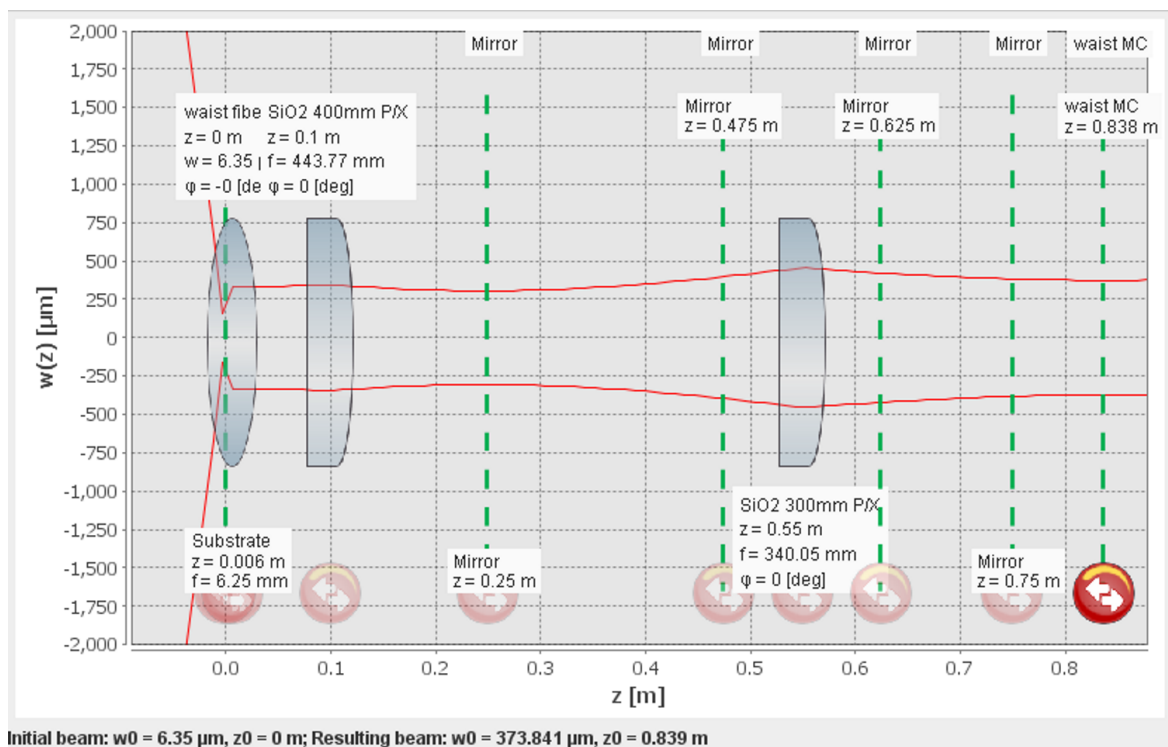
Fig. A.1 Mode matching in the AEI 10 m Prototype tank. Beam profile from the fiber coupling to the mode filter. All components are marked with their position and their beam properties.
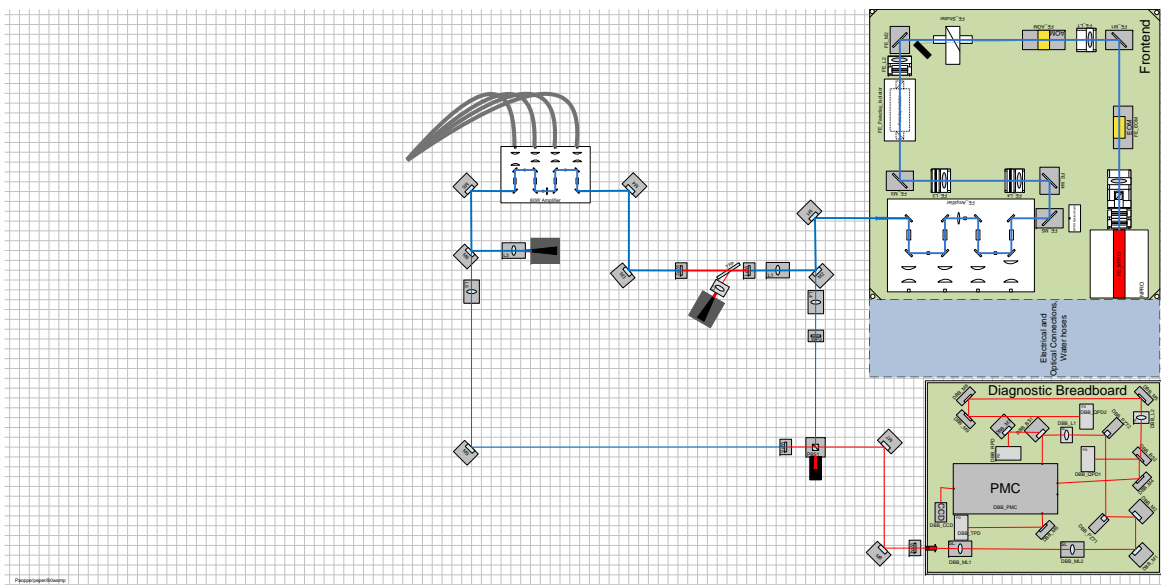
Fig. A.2 Preliminary structure of the experiment at the Engineering Prototype of 35 W amplifier and then two different ways in the DBB. 1 % of the power of the 35 W amplifier is sent directly to the DBB via a power setting after the second mirror. The rest is sent from 70 W amplifier. Again, 1 % of the light is sent to the DBB in a different polarization via its own attenuation unit.
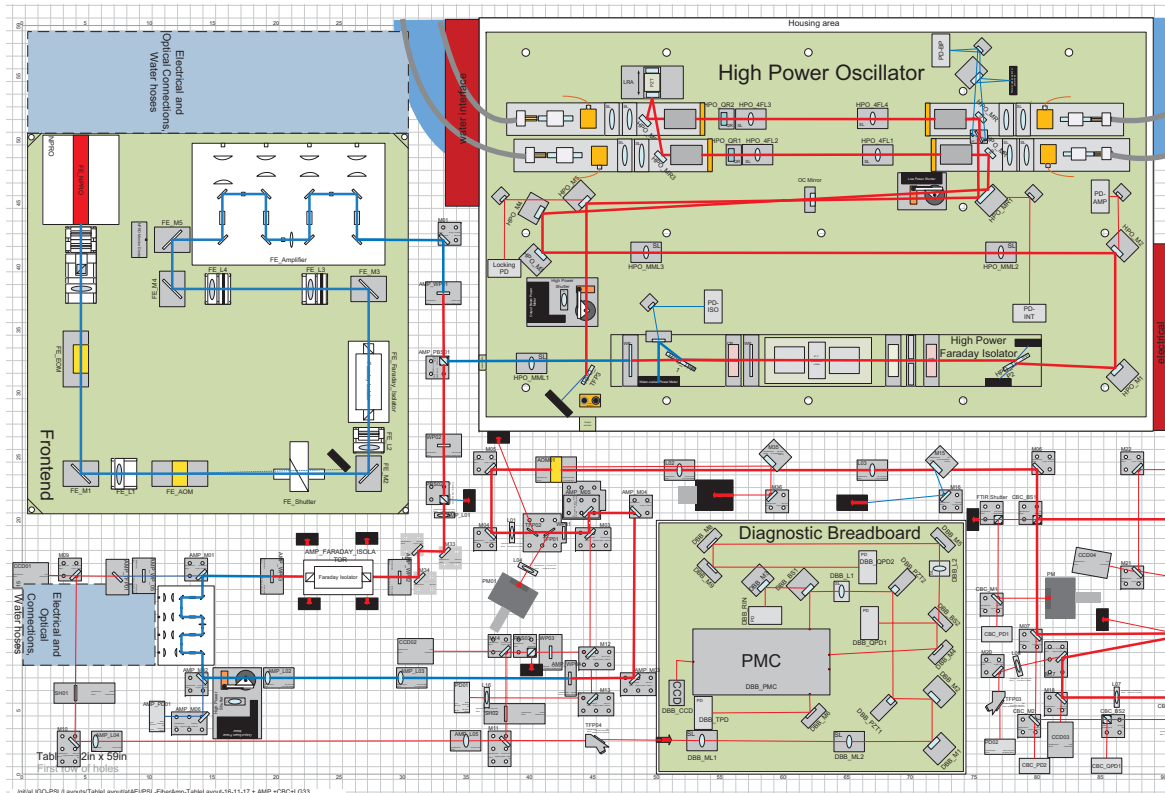
Fig. A.3 Installation of the 70 W amplifier in the aLIGO reference system. First of all, a possibility had to be created that splits the light of the 35 W amplifier between HPO and 70 W amplifier. For this purpose, the last deflection mirror before the HPO was replaced by a polarization beam splitter and a lambda half-plate. The transmitted light is directed into the 70 W amplifier through a Faraday isolator. Behind the amplifier, the light is directed to the high power oscillator via lenses and mirrors. The DBB path of the 35 W amplifier was preserved and is rebuilt behind the 70 W amplifier. Diagnostic measurements are therefore possible for all systems.
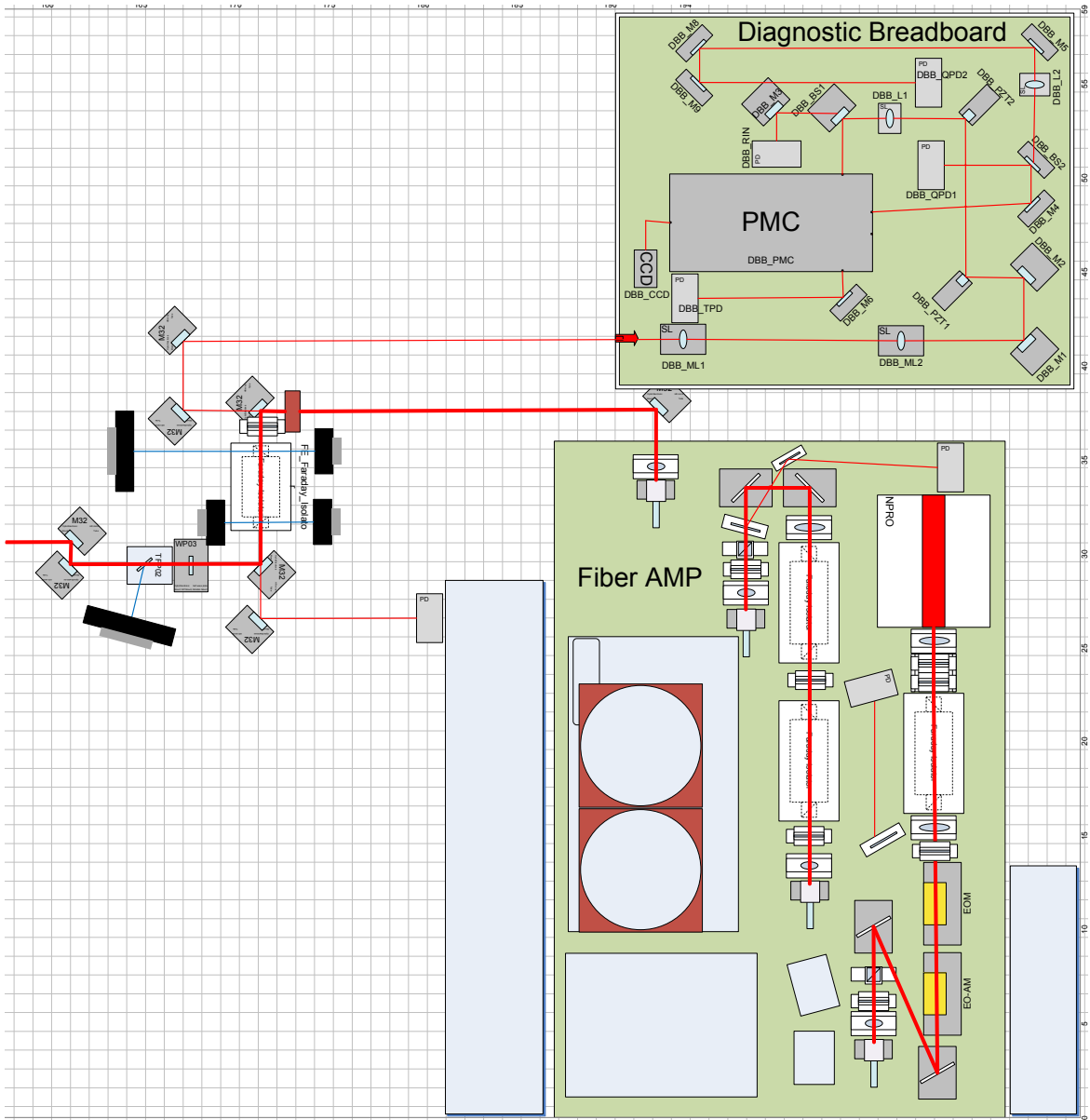
Fig. A.4
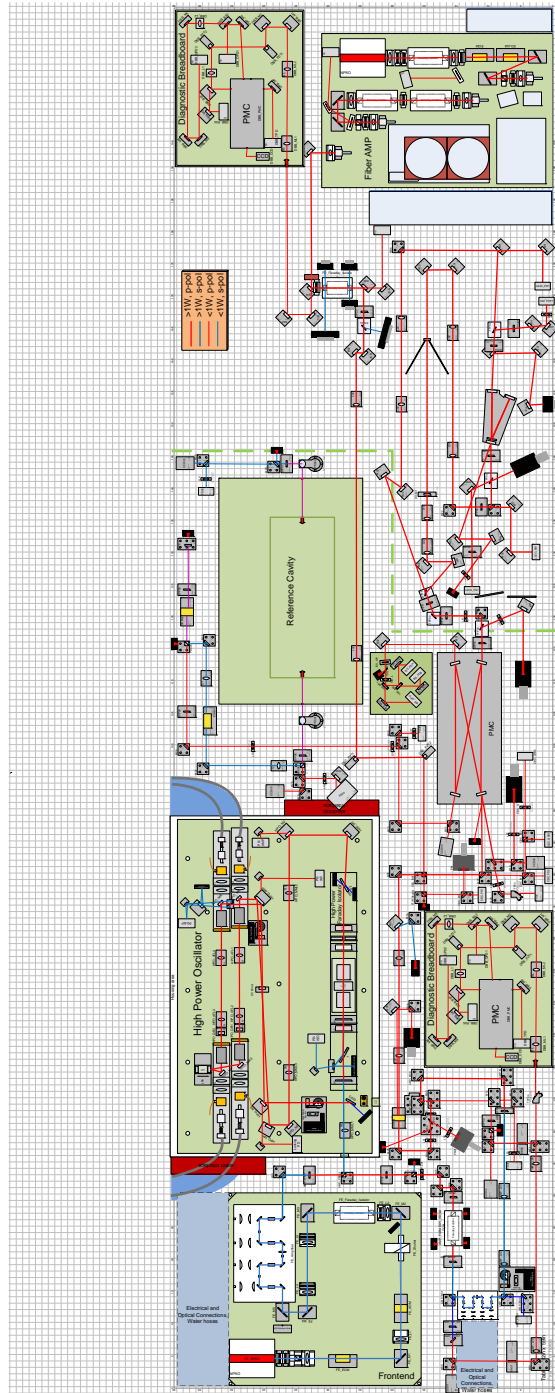
Fig. A.5 Layout of the reference table in AEI Grey room Starting with the 200 W high-power oscillator and the 70 W solid state amplifier. The fiber amplifier can be seen with a DBB.

Fig. A.6 Schematic representation of the temperature controller for temperature stabilization of the two main amplifier coils.

Fig. A.7

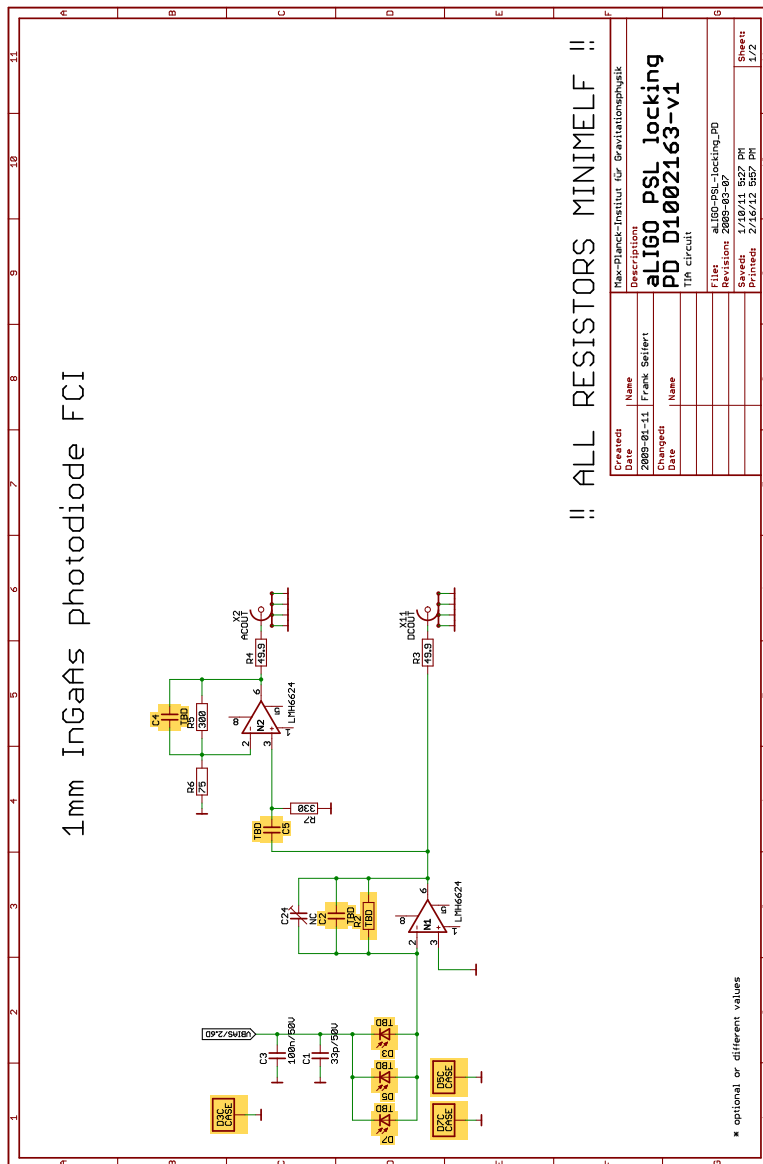# Acknowledgements